MultiCraft

International Journal of Engineering, Science and Technology
Vol. 1, No. 1, 2009, pp. 148-171

INTERNATIONAL JOURNAL OF ENGINEERING, SCIENCE AND TECHNOLOGY

www.ijest-ng.com

Design aids for fixed support reinforced concrete cylindrical shells under uniformly distributed loads

Srinivasan Chandrasekaran[1*], S.K.Gupta[2], Federico Carannante[3]

[1*] *Dept. of Ocean Engineering, Indian Institute of Technology Madras, Chennai 600 036, India*
[2] *Dept. of Civil Engineering, Institute of Technology, Banaras Hindu University, Varanasi, India*
[3] *Dept. of Structural Engineering, University of Naples Federico II, Naples, Italy*
[*] *Corresponding Author: e-mail:drsekaran@iitm.ac.in; Fax: +91-44-22574802*

Abstract

Shells are objects considered as materialization of the curved surface. Despite structural advantages and architectural aesthetics possessed by shells, relative degree of unacquaintance with shell behavior and design is high. Thin shells are examples of strength through form as opposed to strength through mass; their thin cross-section makes them economical due to low consumption of cement and steel as compared to other roof coverings such as slabs. Current study presents design curves for reinforced concrete open barrel cylindrical shells for different geometric parameters. The analysis is done in two parts namely: i) RC shell subjected to uniformly distributed load that remain constant along its length and curvature of the shell surface; and ii) RC shell subjected to uniformly distributed load varying sinusoidally along its length in addition to different symmetric edge loads present along its longitudinal boundaries. Design charts are proposed for easier solution of shell constants after due verification of results obtained from finite element analysis. Expressions for stress resultants proposed in closed form make the design more simple and straightforward; stress resultants plotted at closer intervals of φ can be useful for detailing of reinforcement layout in RC shells. Axial force-bending moment yield interaction studied on shells under uniformly distributed loads show compression failure, initiating crushing of concrete.

Keywords: cylindrical shells; design curves; open barrel; reinforced concrete; stress resultants

1. Introduction

Shells are skin structures by virtue of their geometry and shell action is essentially more towards transmitting the load by direct stresses with relatively small bending stresses. Presence of significant shear makes their behavior different from other roof covering structures; they have remarkable reserve strength with a greater degree-of-freedom in structure layout, shape and architecture, making them virtually impossible to collapse though their supporting structure may collapse (Rericha 1996; Ha-Wong Song *et al.* 2002). A number of procedures are proposed in the literature (see, for example, Flugge 1967) for analyzing the various types of thin shells for ultimate load but experimental evidences, however are not abundant. In many of these procedures, bending stresses are stated to be negligibly small justifying the application of membrane theory for analyzing thin shells, where normal forces are not necessarily tensile. Though behavior of shells to external loads is generally quite complex, thanks to second order equations developed that are sufficient to model the behavior of most civil engineering shell structures (Jacques, 1977). Forces in thin shells are, in a certain sense, statically determinant as they can be determined without referring to elastic property of material used. Linear elastic behavior is applied to provide a direct relationship between stress and strains by which the equilibrium of stress resultant and stress couples could be established. However mathematical models of thin RC shells developed on the interpretation of their physical behavior are difficult to present rationally as the rigorous analysis is extraordinarily complex, resolving to simplification (see, for example, Billington, 1965). These simplifications need extra caution for the design to become conservative. Also, interestingly, load carrying capacity of thin curved shells often exceeds the prediction of even most-refined available analysis. It is therefore commonly accepted that shells (reinforced concrete shells, in particular) are designed on the basis of approximate analysis only, which of course exhibits defects. For example, aircraft impact on containment structures is studied

by employing modal analysis to estimate their elastic response (Prabhakar, 2003). The study approximates shell with uniform thickness in longitudinal and circumferential directions and orthotropic properties are obtained by scaling the Young's modulus values. Wheen and Wheen (2003) studied design and construction principles of a pre-stressed conical concrete tent roof idealizing it as thin pre-tensioned radial circles suspended from a temporary central tower and anchored at the lower ends to a pre-stressed ring beam in a catenary form. They showed that the curved concrete surface, usually a felicitous combination of sound structural form and method of construction leading also to low cost, does not crack when suspended because of radial pre-stressing. Concrete domes, in particular, possess limited membrane stress variations due to soundness in structural form and therefore ideal as all stresses are compressive during construction and in final stages as well (Wheen and Anatharaman, 1998). Example structures presented above for designing/constructing RC shell structures prove the confidence level of researchers in employing relevant approximate theories for analyzing shell structures. This leads to the desire of simplifying the analysis procedure and adding to architectural aesthetics and structural advantages shell possess; the objective is to simplify analysis procedure by means of ready to use design curves and tables. This shall not only promote more construction of such advantageous and safe structures but also improve the confidence level in design offices. However, other studies conducted by the authors emphasize verification of stress resultants at closer intervals of geometric angles at boundaries, in particular, for appropriate detailing of reinforcement in RC shells (see, for example, Chandrasekara *et al.* 2005; Chandrasekaran and Srivastava, 2006). Ramaswamy (1968) discussed limitations and precision of various theories on shell structures and concluded that Flügge's theory is acceptable and can be treated as a bench mark to assess the accuracy of other theories.

2. Objectives and structural idealization

Based on the critical review of literature, main objective of the current study is to develop design curves based on the classical flexural theory for single barrel open cylindrical shells with different geometric parameters; the outcome is to derive the stress resultant estimates that can be readily determined without undergoing detailed computations. Though theory employed is not new but the attempt made to simplify the analysis procedure is relatively new and the analytical solutions proposed in the paper are not present in the literature. As the solution procedure of generic case of shell geometry shall involve complex mathematics, objective of simplifying the design procedure through design curves shall not be fulfilled; hence a particular geometric case of cylindrical shells is only addressed in the present study. Please note that cylindrical shells are commonly used geometry in structural/civil engg applications. With the use of proposed design curves, stress resultants and stress couples can easily be readily determined at the valley, crown or at any desired section for various type of edge loads. This shall be helpful to be employed in design offices while encouraging such new RC shell structures in future and also enhances the confidence of the structural designer. The study employs few structural idealizations namely: i) stress normal to the surface is neglected as thin shell is a curved slab whose thickness is relatively small compared to its other dimensions and radius of curvature; ii) deflections under load are small enough so that its static equilibrium remain affected due to changes in geometry, vide small deflection theorem; iii) linear elastic behavior is assumed in the analysis enabling a direct relationship between stress and strain; iv) for all kinematic relations, any point on the mid surface is considered as unaffected by the shell deformation; as well as v) all points lying normal to the middle surface before deformation lie on the normal after deformation.

3. Mathematical development

Let us consider a cylindrical coordinate system (x,φ,r) and a cylindrical shell with thickness t. The cylindrical shell has the directive along the x-axis and we denote u_x, u_φ, u_r as the displacements along longitudinal (x), circumferential (φ) and radial directions (r), respectively. It is important to note that the displacements, strains and stress functions depend only on two variables namely (φ, x). Figure.1 shows the overall geometry of the shell considered for the study while Figure.2 shows the differential element considered for the analysis. The three strain components $\varepsilon_x, \varepsilon_\varphi$ and $\gamma_{x\varphi}$ of the middle surface and the three curvature changes χ_x, χ_φ and $\chi_{x\varphi}$ can be expressed in terms of the displacement components as given below:

$$\varepsilon_x = \frac{\partial u_x}{\partial x},\ \varepsilon_\varphi = \frac{1}{R}\left(\frac{\partial u_\varphi}{\partial \varphi} - u_r\right),\ \gamma_{x\varphi} = \frac{1}{R}\frac{\partial u_x}{\partial \varphi} + \frac{\partial u_\varphi}{\partial x},$$
$$\phi_x = \frac{\partial^2 u_r}{\partial x^2}, \phi_\varphi = \frac{1}{R^2}\left(\frac{\partial u_\varphi}{\partial \varphi} + \frac{\partial^2 u_r}{\partial \varphi^2}\right),\ \phi_{x\varphi} = \frac{1}{R}\left(\frac{\partial u_\varphi}{\partial x} + \frac{\partial^2 u_r}{\partial x \partial \varphi}\right) \quad (1)$$

Corresponding quantities associated with the strain components and curvatures are the membrane resultant forces $N_x, N_\varphi, N_{x\varphi}$, and resultant moments $M_x, M_\varphi, M_{x\varphi}$, respectively. In addition, resultant shear forces Q_x, Q_φ are also present. The shell is constituted by isotropic material characterized by two elastic constants namely: i) modulus of elasticity, E and ii) poisons modulus ν.

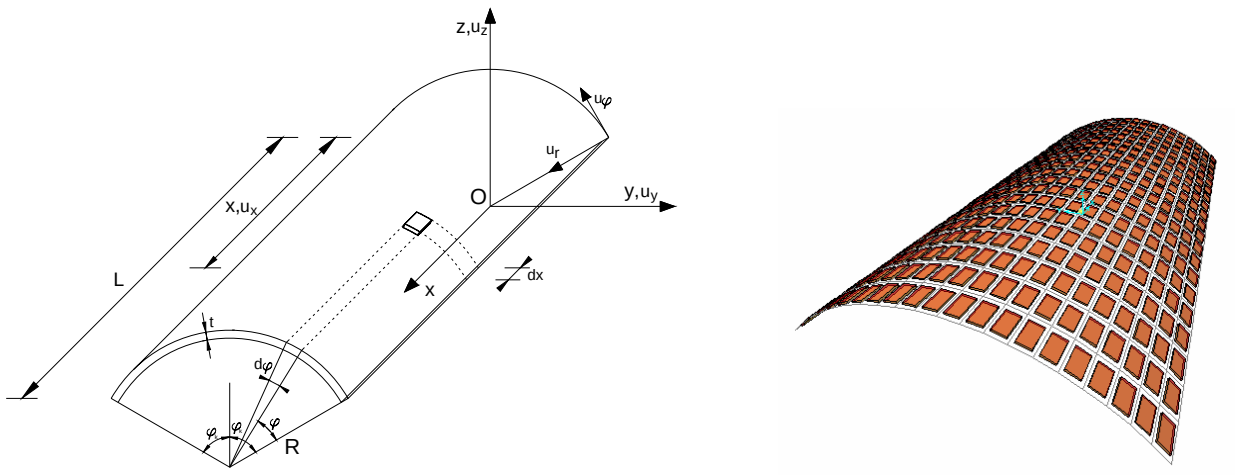

Figure 1. Analytical and FEM Model

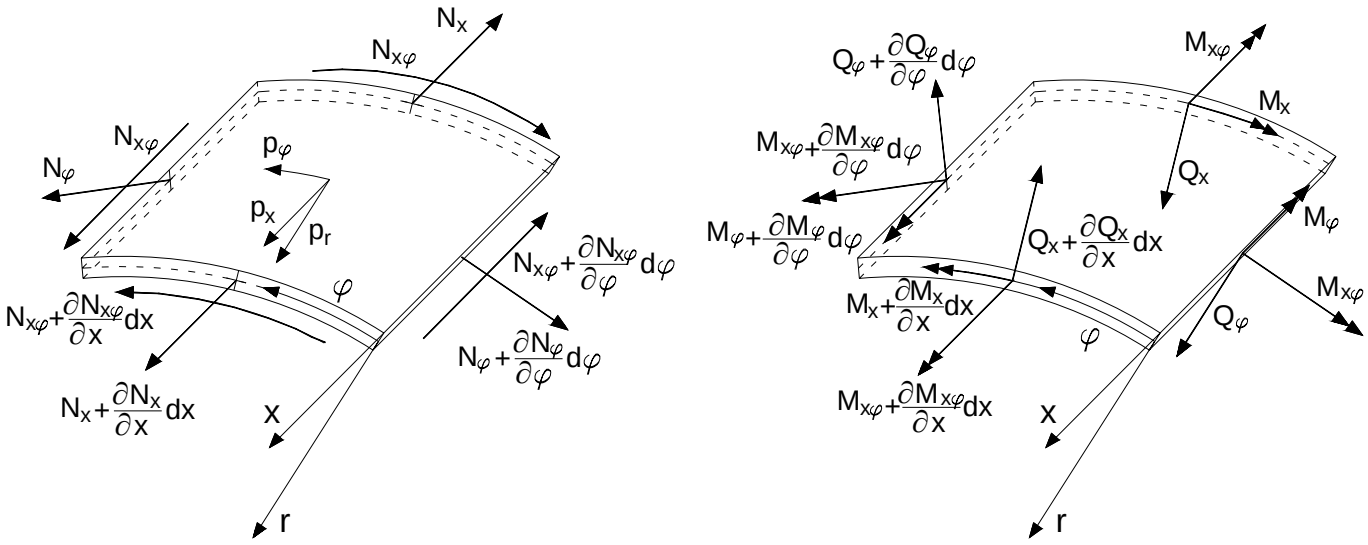

Figure 2. Membrane stresses, moment and shear forces acting on infinitesimal element of shell

Relationships between static quantities and strain/curvature given by the Hooke's law are shown below:

$$N_x = \frac{Et}{1-v^2}\left(\varepsilon_x + v\,\varepsilon_\varphi\right), \quad N_\varphi = \frac{Et}{1-v^2}\left(\varepsilon_\varphi + v\,\varepsilon_x\right), \quad N_{x\varphi} = \frac{Et}{2(1+v)}\gamma_{\varphi x},$$
$$M_x = -\frac{Et^3}{12\left(1-v^2\right)}\left(\chi_x + v\chi_\varphi\right), \quad M_\varphi = -\frac{Et^3}{12\left(1-v^2\right)}\left(\chi_\varphi + v\chi_x\right), \quad M_{x\varphi} = -M_{\varphi x} = \frac{Et^3}{12(1+v)}\chi_{x\varphi} \tag{2}$$

By substituting Eq. (1) in Eq. (2), force-displacement relationships are derived as given below:

$$N_x = \frac{Et}{R\left(1-v^2\right)}\left[R\frac{\partial u_x}{\partial x} + v\left(\frac{\partial u_\varphi}{\partial \varphi} - u_r\right)\right], \quad N_\varphi = \frac{Et}{R\left(1-v^2\right)}\left(vR\frac{\partial u_x}{\partial x} + \frac{\partial u_\varphi}{\partial \varphi} - u_r\right), \quad N_{x\varphi} = \frac{Et}{2(1+v)}\left(\frac{\partial u_\varphi}{\partial x} + \frac{1}{R}\frac{\partial u_x}{\partial \varphi}\right),$$
$$M_x = \frac{Et^3}{12\left(1-v^2\right)}\left[\frac{\partial^2 u_r}{\partial x^2} + \frac{v}{R^2}\left(\frac{\partial u_\varphi}{\partial \varphi} + \frac{\partial^2 u_r}{\partial \varphi^2}\right)\right], \quad M_\varphi = -\frac{Et^3}{12\left(1-v^2\right)}\left[v\frac{\partial^2 u_r}{\partial x^2} + \frac{1}{R^2}\left(\frac{\partial u_\varphi}{\partial \varphi} + \frac{\partial^2 u_r}{\partial \varphi^2}\right)\right], \tag{3}$$
$$M_{x\varphi} = \frac{Et^3}{12(1+v)R}\left(\frac{\partial u_\varphi}{\partial x} + \frac{\partial^2 u_r}{\partial x \partial \varphi}\right) = -M_{\varphi x}$$

For a general case in three dimensions, we can write three equation of equilibrium along x,y and z direction and three equations of moments with respect to the x,y, and z axes. In total there are six equations of equilibrium available for solving eight unknown

functions. If $N_x, N_\varphi, N_{x\varphi}$ are small in comparison with their critical values at which lateral buckling of the shell may occur, their effect on bending becomes negligible; all terms containing the products of the resultant forces or resultant moments with the derivatives of the small displacements can be neglected in the equilibrium equations (Timoshenko and Krieger, 1959). With this hypothesis, equilibrium equations are now reduced to five as given below:

$$\begin{aligned}
&\frac{\partial N_x}{\partial x}R+\frac{\partial N_{\varphi x}}{\partial \varphi}+p_x R=0\\
&\frac{\partial N_{x\varphi}}{\partial x}R+\frac{\partial N_{\varphi}}{\partial \varphi}-Q_{\varphi}+p_{\varphi}R=0\\
&\frac{\partial Q_x}{\partial x}R+\frac{\partial Q_{\varphi}}{\partial \varphi}+N_{\varphi}+p_r R=0\\
&\frac{\partial M_{x\varphi}}{\partial x}R-\frac{\partial M_{\varphi}}{\partial \varphi}+Q_{\varphi}R=0\\
&-\frac{\partial M_x}{\partial x}R-\frac{\partial M_{\varphi x}}{\partial \varphi}+Q_x R=0
\end{aligned} \tag{4}$$

where p_x, p_φ, p_r are the load for unit surface along x-axis, circumferential and radial direction, respectively. Solving last two equations with respect to Q_φ, Q_x and substituting in remain three equations, we finally obtain the three following relationship:

$$\begin{aligned}
&\frac{\partial N_x}{\partial x}R+\frac{\partial N_{\varphi x}}{\partial \varphi}+p_x R=0\\
&\frac{\partial N_{\varphi}}{\partial \varphi}+\frac{\partial N_{x\varphi}}{\partial x}R+\frac{\partial M_{x\varphi}}{\partial x}-\frac{1}{R}\frac{\partial M_{\varphi}}{\partial \varphi}+p_{\varphi}R=0\\
&\frac{\partial^2 M_{\varphi x}}{\partial x\partial \varphi}+\frac{\partial^2 M_x}{\partial x^2}R-\frac{\partial^2 M_{x\varphi}}{\partial x\partial \varphi}+\frac{1}{R}\frac{\partial^2 M_{\varphi}}{\partial \varphi^2}+N_{\varphi}+p_r R=0
\end{aligned} \tag{5}$$

The shear functions have the following expression:

$$\begin{aligned}
Q_\varphi &= -\frac{Et^3}{12R^3(1-\nu^2)}\left[\frac{\partial^2 u_\varphi}{\partial \varphi^2}+\frac{\partial^3 u_r}{\partial \varphi^3}+R^2\left(\frac{\partial^3 u_r}{\partial x^2\partial \varphi}+(1-\nu)\frac{\partial^2 u_\varphi}{\partial x^2}\right)\right]\\
Q_x &= -\frac{Et^3}{12R^2(1-\nu^2)}\left(\frac{\partial^2 u_\varphi}{\partial x\partial \varphi}+\frac{\partial^3 u_r}{\partial x\partial \varphi^2}+R^2\frac{\partial^3 u_r}{\partial x^3}\right)
\end{aligned} \tag{6}$$

Substituting the equations (3) in equations (5), we obtain the equilibrium equation in terms of the unknown displacement functions u_x, u_φ, u_r as given below:

$$\begin{cases}
\dfrac{\partial^2 u_x}{\partial x^2}+\left(\dfrac{1-\nu}{2R}\right)\dfrac{\partial^2 u_x}{\partial \varphi^2}+\left(\dfrac{1+\nu}{2R}\right)\dfrac{\partial^2 u_\varphi}{\partial x\partial \varphi}-\dfrac{\nu}{R}\dfrac{\partial u_r}{\partial x}+\dfrac{p_x\left(1-\nu^2\right)}{Et}=0\\
\dfrac{1+\nu}{2}\dfrac{\partial^2 u_x}{\partial x\partial \varphi}+\left(\dfrac{1-\nu}{2}\right)R\dfrac{\partial^2 u_\varphi}{\partial x^2}+\dfrac{1}{R}\left(\dfrac{\partial^2 u_\varphi}{\partial \varphi^2}-\dfrac{\partial u_r}{\partial \varphi}\right)+\dfrac{t^2}{12R}\left[(1-\nu)\dfrac{\partial^2 u_\varphi}{\partial x^2}+\dfrac{1}{R^2}\dfrac{\partial^2 u_\varphi}{\partial \varphi^2}+\dfrac{\partial^3 u_r}{\partial x^2\partial \varphi}+\dfrac{1}{R^2}\dfrac{\partial^3 u_r}{\partial \varphi^3}\right]+p_\varphi R\left(\dfrac{1-\nu^2}{Et}\right)=0\\
\nu\dfrac{\partial u_x}{\partial x}+\dfrac{1}{R}\dfrac{\partial u_\varphi}{\partial \varphi}-\dfrac{u_r}{R}-\dfrac{t^2}{12}\left[R\dfrac{\partial^4 u_r}{\partial x^4}+\dfrac{2}{R}\dfrac{\partial^4 u_r}{\partial x^2\partial \varphi^2}+\dfrac{1}{R^3}\dfrac{\partial^4 u_r}{\partial \varphi^4}+\dfrac{2-\nu}{R}\dfrac{\partial^3 u_\varphi}{\partial x^2\partial \varphi}+\dfrac{1}{R^3}\dfrac{\partial^3 u_\varphi}{\partial \varphi^3}\right]+p_r R\left(\dfrac{1-\nu^2}{Et}\right)=0
\end{cases} \tag{7}$$

3.1 Analytical solution in closed form for shells under uniform distributed load

Let us consider an open barrel cylindrical shell loaded by uniform distributed load, as seen in Figure 3. The boundaries of the shell along its length are considered as fixed support in the analysis. Stress functions will depend only on one variable, namely φ leading to the following differential equations system:

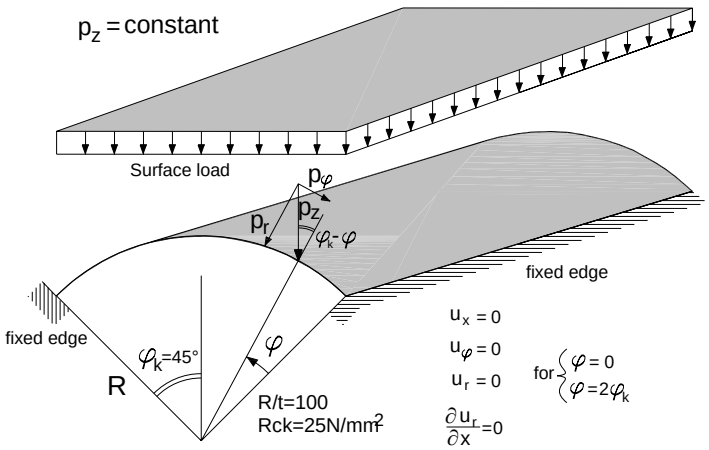

Figure 3. Shell under uniform distributed load

$$\begin{cases} \dfrac{\partial N_x}{\partial x}=0 \;\Rightarrow\; R\dfrac{\partial^2 u_x}{\partial x^2}+v\left(\dfrac{\partial^2 u_\varphi}{\partial\varphi\partial x}-\dfrac{\partial u_r}{\partial x}\right)=0 \\ \dfrac{\partial N_\varphi}{\partial x}=0 \;\Rightarrow\; vR\dfrac{\partial^2 u_x}{\partial x^2}+\dfrac{\partial^2 u_\varphi}{\partial\varphi\partial x}-\dfrac{\partial u_r}{\partial x}=0 \\ \dfrac{\partial N_{x\varphi}}{\partial x}=0 \;\Rightarrow\; \dfrac{\partial^2 u_\varphi}{\partial x^2}+\dfrac{1}{R}\dfrac{\partial^2 u_x}{\partial\varphi\partial x}=0 \\ \dfrac{\partial M_x}{\partial x}=0 \;\Rightarrow\; \dfrac{\partial^3 u_r}{\partial x^3}+\dfrac{v}{R^2}\left(\dfrac{\partial^2 u_\varphi}{\partial\varphi\partial x}+\dfrac{\partial^3 u_r}{\partial\varphi^2\partial x}\right)=0 \\ \dfrac{\partial M_\varphi}{\partial x}=0 \;\Rightarrow\; v\dfrac{\partial^3 u_r}{\partial x^3}+\dfrac{1}{R^2}\left(\dfrac{\partial^2 u_\varphi}{\partial\varphi\partial x}+\dfrac{\partial^3 u_r}{\partial\varphi^2\partial x}\right)=0 \\ \dfrac{\partial M_{x\varphi}}{\partial x}=0 \;\Rightarrow\; \left(\dfrac{\partial^2 u_\varphi}{\partial x^2}+\dfrac{\partial^3 u_r}{\partial x^2\partial\varphi}\right)=0 \end{cases} \Rightarrow \begin{cases} \dfrac{\partial^2 u_x}{\partial x^2}=0 \\ \dfrac{\partial}{\partial x}\left(\dfrac{\partial u_\varphi}{\partial\varphi}-u_r\right)=0 \\ \dfrac{\partial}{\partial x}\left(\dfrac{\partial u_x}{\partial\varphi}+R\dfrac{\partial u_\varphi}{\partial x}\right)=0 \\ \dfrac{\partial^3 u_r}{\partial x^3}=0 \\ \dfrac{\partial}{\partial x\partial\varphi}\left(u_\varphi+\dfrac{\partial u_r}{\partial\varphi}\right)=0, \\ \dfrac{\partial^2}{\partial x^2}\left(u_\varphi+\dfrac{\partial u_r}{\partial\varphi}\right)=0 \end{cases} \tag{8}$$

From the first and fourth equations of the above set of equations, we can derive the following:

$$\begin{aligned} u_x(x,\varphi)&=p_0(\varphi)+p_1(\varphi)x \\ u_r(x,\varphi)&=q_0(\varphi)+q_1(\varphi)x+q_2(\varphi)x^2 \end{aligned} \tag{9}$$

where $p_0(\varphi)$, $p_1(\varphi)$,$q_0(\varphi)$, $q_1(\varphi)$,$q_2(\varphi)$ are unknown functions of variable φ.

By substituting Eq. (9) in the last equation of Eq. (8), we obtain the function $u_\varphi(x,\varphi)$ as given below:

$$u_\varphi(x,\varphi)=h_0(\varphi)+h_1(\varphi)x-\frac{dq_2(\varphi)}{d\varphi}x^2 \tag{10}$$

where $h_0(\varphi)$, $h_1(\varphi)$ are unknown functions of variable φ.

By substituting Eqs (9-10) in Eq. (8), we obtain the following relationships:

$$\begin{aligned} q_1(\varphi)&=C_4\cos\varphi-C_3\sin\varphi \\ q_2(\varphi)&=C_1\cos\varphi+C_2\sin\varphi \\ h_1(\varphi)&=C_3\cos\varphi+C_4\sin\varphi+C_5 \\ p_0(\varphi)&=r\left(C_4\cos\varphi-C_3\sin\varphi\right)+C_7+C_8\varphi \\ p_1(\varphi)&=2r\left(C_1\cos\varphi+C_2\sin\varphi\right)+C_6 \end{aligned} \tag{11}$$

By substituting in Eqs. (9-10), the displacements functions are obtained as given below:

$$\begin{aligned} u_x(x,\varphi) &= C_7 + C_6 x + C_8\varphi + r\cos\varphi(C_4 + 2C_1 x) - r\sin\varphi(C_3 - 2C_2 x) \\ u_\varphi(x,\varphi) &= h_0(\varphi) + x\sin\varphi(C_1 x + C_4) + x\cos\varphi(C_3 - C_2 x) + C_5 \\ u_r(x,\varphi) &= q_0(\varphi) + x\cos\varphi(C_1 x + C_4) - x\sin\varphi(C_3 - C_2 x) \end{aligned} \tag{12}$$

The uniform distributed load applied on surface of the shell is resolved into components along (x,φ,r) as given below:

$$\begin{cases} p_x = 0 \\ p_\varphi = -p\ \sin(\varphi_k - \varphi) \\ p_r = p\ \cos(\varphi_k - \varphi) \end{cases} \tag{13}$$

where φ_k is total shell angle in radians. By substituting Eq.(12) in equilibrium Eq. (7), the first condition is verified. Further, by substituting the function $q_0(\varphi)$ with its first derivative, the third equation of Eq. (12) becomes:

$$u_r(x,\varphi) = \frac{dq_0(\varphi)}{d\varphi} + x\cos\varphi(C_1 x + C_4) - x\sin\varphi(C_3 - C_2 x) \tag{14}$$

Now, the second and third equations of Eq. (7) become:

$$\begin{aligned} &Et\left[\frac{d^4 q_0(\varphi)}{d\varphi^4}t^2 + \left(12R^2 + t^2\right)\frac{d^2 h_0(\varphi)}{d\varphi^2} - 12R^2\frac{d^2 q_0(\varphi)}{d\varphi^2}\right] \\ &+ 2ER^2 vt\left(12R^2 + t^2\right)(C_2\cos\varphi - C_1\sin\varphi) - 12pR^4\left(1 - v^2\right)\sin(\varphi - \varphi_k) = 0 \end{aligned} \tag{15}$$

$$\begin{aligned} &12R^2 Et\left[\frac{dq_0(\varphi)}{d\varphi} - \frac{dh_0(\varphi)}{d\varphi} + t^2\left(\frac{d^3 h_0(\varphi)}{d\varphi^3} + \frac{d^5 q_0(\varphi)}{d\varphi^5}\right)\right] \\ &- 2ER^2 vt\left[6RC_6 + \left(12R^2 + t^2\right)(C_2\cos\varphi - C_1\sin\varphi)\right] - 12pR^4\left(1 - v^2\right)\cos(\varphi - \varphi_k) = 0 \end{aligned} \tag{16}$$

By integrating Eq. (15) twice we get:

$$\begin{aligned} h_0(\varphi) &= 2R^2 v(C_2\cos\varphi - C_1\sin\varphi) + \frac{12p\,R^4\left(1 - v^2\right)\sin(\varphi - \varphi_k)}{Et\left(12R^2 + t^2\right)} \\ &+ \frac{1}{\left(12R^2 + t^2\right)}\left[12R^2 q_0(\varphi) - t^2\frac{d^2 q_0(\varphi)}{d\varphi^2}\right] + C_9\varphi + C_{10} \end{aligned} \tag{17}$$

By substituting in Eq. (16) we get the following differential equation in $q_0(\varphi)$:

$$Et^3\left[\frac{dq_0(\varphi)}{d\varphi} + 2\frac{d^3 q_0(\varphi)}{d\varphi^3} + \frac{d^5 q_0(\varphi)}{d\varphi^5}\right] - \left(12R^2 + t^2\right)\left[Et(C_9 + C_6 Rv) + 2pR^2\left(1 - v^2\right)\cos(\varphi - \varphi_k)\right] = 0 \tag{18}$$

By solving, function $q_0(\varphi)$ is obtained and is given as below:

$$\begin{aligned} q_0(\varphi) &= \frac{pR^2\left(12R^2 + t^2\right)\left(v^2 - 1\right)\left[8\varphi\cos\varphi + \left(2\varphi^2 - 11\right)\sin\varphi\right]\cos\varphi_k}{8Et^3} + \frac{\left(12R^2 + t^2\right)(C_9 + C_6 Rv)\varphi + (C_{11} + C_{14} + \varphi C_{12})\sin\varphi}{t^2} \\ &+ \frac{pR^2\left(12R^2 + t^2\right)\left(1 - v^2\right)\left[\left(2\varphi^2 - 11\right)\cos\varphi - 8\varphi\sin\varphi\right]\sin\varphi_k}{8Et^3} + (C_{12} - C_{13} - \varphi C_{14})\cos\varphi + C_{15} \end{aligned} \tag{19}$$

Now the hypothesis is verified to satisfy the equilibrium and compatibility conditions. By substituting Eq. (19) and Eq. (17) in Eq. (12), displacement functions u_x, u_φ, u_r are obtained in a closed form. The integration constants $C_{i=1,2,\ldots,14}$ (the constant C_{15} is not present in displacement function as the function u_r is considered as a derivative of is present the derivate of function $q_0(\varphi)$ given by Eq. (14)) are determined by imposing the boundary conditions at fixed supports and using polynomial identity rule. The following sets of algebraic equations are obtained.

$$\begin{cases} u_x(x,\varphi=0)=0 & \forall x \Rightarrow p_0(\varphi=0)=0;\ p_1(\varphi=0)=0 \\ u_x(x,\varphi=2\varphi_k)=0 & \forall x \Rightarrow p_0(\varphi=2\varphi_k)=0;\ p_1(\varphi=2\varphi_k)=0 \\ u_\varphi(x,\varphi=0)=0 & \forall x \Rightarrow h_0(\varphi=0)=0;\ h_1(\varphi=0)=0;\ \dfrac{dq_2(\varphi=0)}{d\varphi}=0 \\ u_\varphi(x,\varphi=2\varphi_k)=0 & \forall x \Rightarrow h_0(\varphi=2\varphi_k)=0;\ h_1(\varphi=2\varphi_k)=0;\ \dfrac{dq_2(\varphi=2\varphi_k)}{d\varphi}=0 \\ u_r(x,\varphi=0)=0 & \forall x \Rightarrow q_0(\varphi=0)=0;\ q_1(\varphi=0)=0;\ q_2(\varphi=0)=0 \\ u_r(x,\varphi=2\varphi_k)=0 & \forall x \Rightarrow q_0(\varphi=2\varphi_k)=0;\ q_1(\varphi=2\varphi_k)=0;\ q_2(\varphi=2\varphi_k)=0 \\ \dfrac{du_r}{d\varphi}(x,\varphi=0)=0 & \forall x \Rightarrow \dfrac{dq_0}{d\varphi}(\varphi=0)=0;\ \dfrac{dq_1}{d\varphi}(\varphi=0)=0;\ \dfrac{dq_2}{d\varphi}(\varphi=0)=0 \\ \dfrac{du_r}{d\varphi}(x,\varphi=2\varphi_k)=0 & \forall x \Rightarrow \dfrac{dq_0}{d\varphi}(\varphi=2\varphi_k)=0;\ \dfrac{dq_1}{d\varphi}(\varphi=2\varphi_k)=0;\ \dfrac{dq_2}{d\varphi}(\varphi=2\varphi_k)=0 \end{cases} \tag{20}$$

It can be easily seen from the above that there are only 14 independent equations (as same as the integration constants to be determined); the remaining are linearly dependent ones.

$$C_{i=1,2,\ldots 8}=0,\quad C_9=\frac{48\beta t^2R^2\left[\left(t^2\left(8\varphi_k^2-3\right)+12R^2\left(8\varphi_k^2-1\right)\right)\cos\varphi_k+3\left(4R^2+t^2\right)\left(\cos3\varphi_k-4\varphi_k\sin\varphi_k\right)\right]}{\left(12R^2+t^2\right)} \tag{21}$$

$$C_{10}=\frac{-48\beta R^2\varphi_k\left[\left(12R^2+t^2\right)\left(t^2\left(8\varphi_k^2-3\right)+12R^2\left(8\varphi_k^2-1\right)\right)\cos\varphi_k-3\left(48R^4+16R^2t^2+t^4\right)\left(4\varphi_k\sin\varphi_k-\cos3\varphi_k\right)\right]}{\left(12R^2+t^2\right)} \tag{22}$$

$$C_{11}=-6\beta\begin{bmatrix}2\cos\varphi_k\left(t^4\varphi_k^2+24R^4\left(22\varphi_k^2-5\right)+2R^2t^2\left(28\varphi_k^2-9\right)\right)\\+12R^2\cos3\varphi_k+\varphi_k\sin\varphi_k\left(\cos2\varphi_k\left(12R^2+t^2\right)+t^4-240R^4-72R^2t^2\right)\end{bmatrix} \tag{23}$$

$$C_{12}=4\beta\begin{bmatrix}\left(12R^2+t^2\right)^2\varphi_k\left(\left(1+4\varphi_k^2\right)\cos\varphi_k-\cos3\varphi_k\right)\\+4\sin\varphi_k\left(\left(12R^2+t^2\right)^2\varphi_k^2+6R^2\left(36R^2+5t^2\right)\cos2\varphi_k-6\left(36R^4+5R^2t^2\right)\right)\end{bmatrix} \tag{24}$$

$$\begin{aligned}C_{13}=&-2\beta\varphi_k\cos\varphi_k\left(12R^2+t^2\right)^2\left(3+8\varphi_k^2-3\cos2\varphi_k\right)\\&-12\beta\left[\sin\varphi_k\left(\left(12R^2+t^2\right)^2\varphi_k^2-18R^2\left(20R^2+3t^2\right)\right)+6R^2\left(20R^2+3t^2\right)\sin3\varphi_k\right]\end{aligned} \tag{25}$$

$$C_{14}=8\beta\varphi_k\sin\varphi_k\left(12R^2+t^2\right)^2\left[\frac{12R^2\left(2\varphi_k^2-5\right)+t^2\left(2\varphi_k^2-1\right)}{\left(12R^2+t^2\right)}-\cos2\varphi_k\right]+96R^2\beta\left(36R^2+5t^2\right)\sin2\varphi_k\sin\varphi_k \tag{26}$$

where $\beta=\dfrac{pR^2\left(1-v^2\right)}{16Et^3\left[2t^2\varphi_k^2+24R^2\left(\varphi_k^2-1\right)+24R^4\cos2\varphi_k+\left(12R^2+t^2\right)\varphi_k\sin2\varphi_k\right]}$

Substituting the integration constants in the displacement function, we get the following displacement functions:

$$u_x=0 \tag{27}$$

$$\begin{aligned}u_\varphi=&C_{10}+C_9\varphi\left(\frac{12R^2+t^2}{t^2}\right)-\frac{\left[C_{12}\left(t^2-12R^2\right)+\left(12R^2+t^2\right)\left(C_{13}+C_{14}\varphi\right)\right]\cos\varphi}{12R^2+t^2}+\frac{12pR^4\left(v^2-1\right)\varphi\cos\left(\varphi-\varphi_k\right)}{Et^3}\\&+\frac{\left[12R^2\left(C_{11}+C_{14}\right)+t^2\left(C_{11}-C_{14}\right)+C_{12}\varphi\left(12R^2+t^2\right)\right]\sin\varphi}{12R^2+t^2}\\&+\frac{pR^2\left(v^2-1\right)\left[t^4-1584R^4-216R^2t^2+2\varphi^2\left(12R^2+t^2\right)\right]\sin\left(\varphi-\varphi_k\right)}{8Et^3\left(12R^2+t^2\right)}\end{aligned} \tag{28}$$

$$u_r = \frac{pR^2\left(12R^2+t^2\right)\left(v^2-1\right)\left[\left(2\varphi^2-3\right)\cos\varphi-4\varphi\sin\varphi\right]\cos\varphi_k}{8Et^3} + \left(\frac{12R^2+t^2}{t^2}\right)\left[C_9+pR^2\left(v^2-1\right)\sin\varphi_k\left(4\varphi\cos\varphi+\left(2\varphi^2-3\right)\sin\varphi\right)\right]+\left(C_{11}+C_{12}\varphi\right)\cos\varphi+\left(C_{13}+C_{14}\varphi\right)\sin\varphi \tag{29}$$

The stress functions are given by:

$$\begin{aligned}
&M_{x\varphi}=0,\ M_{\varphi x}=0,\ N_{x\varphi}=0,\ Q_x=0,\ N_x=vN_\varphi, M_x=vM_\varphi\\
&N_\varphi = 4\omega Et^3\left(C_{14}\cos\varphi-C_{12}\sin\varphi\right)+p\omega R^2\left(v^2-1\right)\begin{bmatrix}\cos\varphi_k\left(\left(12R^2-t^2\right)\cos\varphi-2\left(12R^2+t^2\right)\varphi\sin\varphi\right)\\+\left(2\left(12R^2+t^2\right)\varphi\cos\varphi+\left(12R^2-t^2\right)\sin\varphi\right)\sin\varphi_k\end{bmatrix}\\
&M_\varphi = \frac{\omega Et}{6R}\left[C_9\left(12R^2+t^2\right)^2+24R^2t^2\left(C_{14}\cos\varphi-C_{12}\sin\varphi\right)\right]\\
&\quad+p\omega R^3\left(v^2-1\right)\left[\sin\varphi_k\left(2\left(12R^2+t^2\right)\varphi\cos\varphi-3\left(4R^2+t^2\right)\sin\varphi\right)-\cos\varphi_k\left(3\left(4R^2+t^2\right)\cos\varphi+2\left(12R^2+t^2\right)\varphi\sin\varphi\right)\right]\\
&Q_\varphi = -4\omega Et^3\left(C_{12}\cos\varphi+C_{14}\sin\varphi\right)+pR^2\left(1-v^2\right)\begin{bmatrix}\cos\varphi_k\left(2\left(12R^2+t^2\right)\varphi\cos\varphi+\left(12R^2-t^2\right)\sin\varphi\right)\\-\sin\varphi_k\left(\left(12R^2-t^2\right)\cos\varphi-2\left(12R^2+t^2\right)\varphi\sin\varphi\right)\end{bmatrix}
\end{aligned} \tag{30}$$

where $\omega=\dfrac{1}{2R\left(12R^2+t^2\right)\left(v^2-1\right)}$

3.2 Analytical solution in closed form for shells under edge loads

The open barrel RC cylindrical shell in now analyzed under uniformly distributed surface load varying sinusoidal in addition to the edge loads. Bellington (1965) presented the general equations of equilibrium under certain assumptions to simplify the stress functions. Poisson's modulus is neglected in this treatment to get the following relationships:

$$N_x=\frac{Et}{R}\frac{\partial u_x}{\partial x},\quad N_\varphi=\frac{Et}{R}\left(\frac{\partial u_\varphi}{\partial\varphi}-u_r\right),\quad N_{x\varphi}=\frac{Et}{2}\left(\frac{\partial u_\varphi}{\partial x}+\frac{1}{R}\frac{\partial u_x}{\partial\varphi}\right) \tag{31a}$$

$$M_x=\frac{Et^3}{12}\frac{\partial^2 u_r}{\partial x^2},\ M_\varphi=-\frac{Et^3}{12R^2}\left(\frac{\partial u_\varphi}{\partial\varphi}+\frac{\partial^2 u_r}{\partial\varphi^2}\right),\ M_{x\varphi}=-M_{\varphi x}=\frac{Et^3}{12R}\frac{\partial}{\partial x}\left(u_\varphi+\frac{\partial u_r}{\partial\varphi}\right) \tag{31b}$$

$$Q_\varphi=-\frac{Et^3}{12R^3}\left[\frac{\partial^2}{\partial\varphi^2}\left(u_\varphi+\frac{\partial u_r}{\partial\varphi}\right)+R^2\frac{\partial^2}{\partial x^2}\left(\frac{\partial u_r}{\partial\varphi}+u_\varphi\right)\right],\quad Q_x=-\frac{Et^3}{12R^2}\frac{\partial}{\partial x}\left[\frac{\partial}{\partial\varphi}\left(u_\varphi+\frac{\partial u_r}{\partial\varphi}\right)+R^2\frac{\partial^2 u_r}{\partial x^2}\right] \tag{31c}$$

In equations (31b), terms of radial displacement u_φ are neglected and Q_φ terms in Eq. (4) are also dropped. By utilizing namely: i) equilibrium equations given by Eq. (4); ii) relationships given by Eq. (31); as well as the compatibility conditions between the displacement components and stresses forces, the elastic problem is now reduced in to a single eighth order partial differential equation with displacement along the radial direction as the only unknown. The modified differential equation is given by:

$$\left(\frac{Et^3}{12}\right)\nabla^8 u_r+\left(\frac{Et}{r^2}\right)\frac{\partial^4 u_r}{\partial x^4}=\nabla^4 p_z+\frac{1}{r^3}\frac{\partial^3 p_x}{\partial x\partial\varphi^2}-\frac{1}{r^2}\frac{\partial}{\partial\varphi}\left(\frac{\partial^2 p_\varphi}{\partial x^2}+\frac{1}{r^2}\frac{\partial^2 p_\varphi}{\partial\varphi^2}\right) \tag{32}$$

Where the differential operator $\nabla^8 u_r$ and $\nabla^4 p_r$ are given by the following expressions:

$$\begin{aligned}
\nabla^8 u_r &= \frac{\partial^8 u_r}{\partial x^8}+\frac{4}{r^2}\frac{\partial^8 u_r}{\partial x^6\partial\varphi^2}+\frac{6}{r^4}\frac{\partial^8 u_r}{\partial x^4\partial\varphi^4}+\frac{4}{r^6}\frac{\partial^8 u_r}{\partial x^2\partial\varphi^6}+\frac{1}{r^8}\frac{\partial^8 u_r}{\partial\varphi^8}\\
\nabla^4 p_r &= \frac{\partial^4 p_r}{\partial x^4}+\frac{2}{r^2}\frac{\partial^4 p_r}{\partial x^2\partial\varphi^2}+\frac{1}{r^4}\frac{\partial^4 p_r}{\partial\varphi^4}
\end{aligned} \tag{33}$$

Let the shell be subjected to surface load 'p' that is distributed uniformly over the shell surface and also varying sinusoidal along its length. The load can be resolved into its components along longitudinal, circumferential and radial directions as given below:

$$\begin{cases} p_x = 0 \\ p_\varphi = -p\ \sin(\varphi_k - \varphi)\ \sin\left(\dfrac{\pi x}{L}\right) \\ p_r = p\ \cos(\varphi_k - \varphi)\ \sin\left(\dfrac{\pi x}{L}\right) \end{cases} \tag{34}$$

where, p = load per unit surface area of the shell surface and L is the span of shell. Equilibrium equations given by Eq. (4) can be satisfied by a particular integral of the form:

$$u_r(x,\varphi) = C_0\ \cos(\varphi_k - \varphi)\ \sin\left(\frac{\pi x}{L}\right) \tag{35}$$

By substituting, the value of constant C_0 that depends on the geometric parameters of the shell is determined as:

$$C_0 = \frac{12L^4 p R^4 \left(2L^4 + 4L^2\pi^2R^2 + \pi^4R^4\right)}{Et\left[t^2\left(L^2 + \pi^2R^2\right)^4 + 12L^4\pi^4R^6\right]} \tag{36}$$

Further by substituting C_0 at any desired section, Eq. (35) gives the displacement in terms of load and geometric characteristics of the reinforced concrete shell. However, particular integral of Eq. (35) does not provide the complete solution and hence complimentary function of Eq. (32) is now considered. Equating the RHS of Eq. (32) to zero, the complimentary function assumes the following form:

$$u_r(x,\varphi) = \sum_{n=1,3,5..}^{\infty} A_m e^{M\varphi} \sin\left(\frac{\pi x}{L}\right) \tag{37}$$

where, A_m represents the eight arbitrary constants depending on the longitudinal boundary conditions and M (in $e^{M\Phi}$) represents the corresponding roots. Variation of $u_r(x,\varphi)$ along the longitudinal boundary can be described by Fourier series considering only the first term of the series. By substituting Eq. (37) in homogenous form of Eq. (32), roots M are determined. On substitution, we get:

$$\left(\frac{M^2}{R^2} - k^2\right)^4 + \frac{12\pi^4}{R^2t^2L^4} = 0 \tag{38}$$

where $k = \dfrac{\pi}{L}$. Eq. (38) in now expressed as:

$$\left(M^2 - k^2R^2\right)^4 + 4Q^8 = 0 \tag{39}$$

where,

$$Q^8 = \frac{3k^4R^6}{t^2},\quad Q = \sqrt{\frac{\pi}{L}}\sqrt[4]{\frac{r^3\sqrt{3}}{t}} \tag{40}$$

By introducing the constant $\gamma = \dfrac{k^2R^2}{Q}$, Eq. (39) is rewritten as:

$$M^2 = Q^2\left(\gamma \pm \sqrt{2i}\right) \tag{41}$$

By applying the Euler's equation, Eq. (41) becomes:

$$M^2 = Q^2\left(\gamma \pm 1 \pm i\right) \tag{42}$$

By solving, we obtain the follows roots:

$$M_1 = \pm(\alpha_1 \pm \beta_1),\ M_2 = \pm(\alpha_2 \pm \beta_2) \tag{43}$$

where,

$$\begin{aligned} \alpha_1 &= Q\sqrt{\frac{\sqrt{(1+\gamma)^2+1}+(1+\gamma)}{2}}, & \alpha_2 &= Q\sqrt{\frac{\sqrt{(1-\gamma)^2+1}-(1-\gamma)}{2}}, \\ \beta_1 &= Q\sqrt{\frac{\sqrt{(1+\gamma)^2+1}-(1+\gamma)}{2}}, & \beta_2 &= Q\sqrt{\frac{\sqrt{(1-\gamma)^2+1}+(1-\gamma)}{2}}, \end{aligned} \tag{44}$$

Now, the complimentary function of Eq. (32) is given by:

$$u_r(x,\varphi)=\begin{bmatrix} A_1e^{(\alpha_1+i\beta_1)\varphi}+B_1e^{(\alpha_1-i\beta_1)\varphi}+A_2e^{(\alpha_2+i\beta_2)\varphi}+B_2e^{(\alpha_2-i\beta_2)\varphi}+ \\ +A_3e^{-(\alpha_1+i\beta_1)\varphi}+B_3e^{-(\alpha_1-i\beta_1)\varphi}+A_4e^{-(\alpha_2+i\beta_2)\varphi}+B_4e^{-(\alpha_2-i\beta_2)\varphi} \end{bmatrix}\sin\left(\frac{\pi x}{L}\right) \tag{45}$$

For $u_r(x,\varphi)$ to be real, the integration constants A_i, B_i $(i=1,2,3,4)$ must be complex; by recalling the integration constants, the displacement function $u_r(x,\varphi)$ is written as:

$$u_r=\begin{bmatrix} (D_1\cos\beta_1\varphi+D_2\sin\beta_1\varphi)e^{\alpha_1\varphi}+(D_3\cos\beta_1\varphi+D_4\sin\beta_1\varphi)e^{-\alpha_1\varphi} \\ +(D_5\cos\beta_2\varphi+D_6\sin\beta_2\varphi)e^{\alpha_2\varphi}+(D_7\cos\beta_2\varphi+D_8\sin\beta_2\varphi)e^{-\alpha_2\varphi} \end{bmatrix}\sin\left(\frac{\pi x}{L}\right) \tag{46}$$

where $D_i\,(i=1,2,3,4,5,6,7,8)$ are integration constants. The final solution is the sum of particular integral given by Eq. (35) and complementary function given by Eq. (46). By substituting in Eq. (31) and utilizing the equilibrium conditions given by Eq. (4), we obtain the stress functions as follows:

$$N_\varphi=\frac{Et^3}{12}\left(R\frac{\partial^4u_r}{\partial x^4}+\frac{2}{R}\frac{\partial^4u_r}{\partial x^2\partial\varphi^2}+\frac{1}{R^3}\frac{\partial^4u_r}{\partial\varphi^4}\right)-p_zR \tag{47}$$

$$N_{x\varphi}=\int\left[-\frac{Et^3}{12}\left(\frac{\partial^5u_r}{\partial x^4\partial\varphi}+\frac{2}{R^2}\frac{\partial^5u_r}{\partial x^2\partial\varphi^3}+\frac{1}{R^4}\frac{\partial^4u_r}{\partial\varphi^5}\right)+\frac{\partial p_r}{\partial\varphi}-p_\varphi\right]dx \tag{48}$$

$$N_x=\int\int\left[\frac{Et^3}{12R}\left(\frac{\partial^6u_r}{\partial x^4\partial\varphi^2}+\frac{2}{R^2}\frac{\partial^6u_r}{\partial x^2\partial\varphi^4}+\frac{1}{R^4}\frac{\partial^6u_r}{\partial\varphi^6}\right)-\frac{\partial^2p_r}{R\partial\varphi^2}+\frac{\partial p_\varphi}{R\partial\varphi}-\frac{\partial p_x}{R\partial x}\right]dxdx \tag{49}$$

$$Q_x=-\frac{Et^3}{12}\left(\frac{\partial^3u_r}{\partial x^3}+\frac{1}{R^2}\frac{\partial^3u_r}{\partial x\partial\varphi^2}\right) \tag{50}$$

$$Q_\varphi=-\frac{Et^3}{12R}\left(\frac{1}{R^2}\frac{\partial^3u_r}{\partial\varphi^3}+\frac{\partial^3u_r}{\partial x^2\partial\varphi}\right) \tag{51}$$

By introducing the following vector, displacement function can be written in more compact form:

$$\bar{\omega}=\begin{bmatrix}\bar{\omega}_1e^{\alpha_1\varphi}\\ \bar{\omega}_1e^{-\alpha_1\varphi}\\ \bar{\omega}_2e^{\alpha_2\varphi}\\ \bar{\omega}_2e^{-\alpha_2\varphi}\end{bmatrix}\qquad \text{where}\quad \bar{\omega}_1=\begin{bmatrix}\cos(\beta_1\varphi)\\ \sin(\beta_1\varphi)\end{bmatrix},\ \bar{\omega}_2=\begin{bmatrix}\cos(\beta_2\varphi)\\ \sin(\beta_2\varphi)\end{bmatrix} \tag{52}$$

$$u_r(x,\varphi)=\left[C_0\cos(\varphi_k-\varphi)+\bar{\omega}\cdot\bar{D}\right]\sin\left(\frac{\pi x}{L}\right) \tag{53}$$

where $\bar{D}=[D_1,D_2,.....,D_8]^T$. In explicit form the stress functions are given by:

$$\begin{aligned}
M_x,M_\varphi,N_x,N_\varphi&=\frac{Et^3}{12}\left[H_0\cos(\varphi_k-\varphi)+\bar{\omega}\cdot\left([\Gamma]\cdot\bar{D}\right)\right]\sin\left(\frac{\pi x}{L}\right)\\
M_{x\varphi},N_{x\varphi}&=\frac{Et^3}{12}\left[H_0\sin(\varphi_k-\varphi)+\bar{\omega}\cdot\left([\Gamma]\cdot[\lambda]\cdot\bar{D}\right)\right]\cos\left(\frac{\pi x}{L}\right)\\
Q_x&=\frac{Et^3}{12}\left[H_0\cos(\varphi_k-\varphi)+\bar{\omega}\cdot\left([\Gamma]\cdot\bar{D}\right)\right]\cos\left(\frac{\pi x}{L}\right)\\
Q_\varphi&=\frac{Et^3}{12}\left[H_0\sin(\varphi_k-\varphi)+\bar{\omega}\cdot\left([\Gamma]\cdot[\lambda]\cdot\bar{D}\right)\right]\sin\left(\frac{\pi x}{L}\right)
\end{aligned} \tag{54}$$

where H_0 assumes different values for different stress functions as given below:

$$H_0 = \begin{cases} \dfrac{\pi^2 C_0}{L^2} & \text{for } M_x \\ \dfrac{C_0}{R^2} & \text{for } M_\varphi \\ \dfrac{\left(L^2+\pi^2R^2\right)^2 C_0}{L^2\pi^2R^5} - \dfrac{24pL^2}{Et^3\pi^2R} & \text{for } N_x \\ \dfrac{\left(L^2+\pi^2R^2\right)^2 C_0}{L^4R^3} - \dfrac{12pR}{Et^3} & \text{for } N_\varphi \\ \dfrac{\pi C_0}{RL} & \text{for } M_{x\varphi} \\ \dfrac{\left(\pi^2R^2+L^2\right)^2 C_0}{\pi L^3R^4} - \dfrac{24p}{\pi L^3 Et^3} & \text{for } N_{x\varphi} \\ \dfrac{\pi\left(L^2+\pi^2R^2\right)C_0}{L^3R^2} & \text{for } Q_x \\ \dfrac{\left(L^2+\pi^2R^2\right)C_0}{L^2R^3} & \text{for } Q_\varphi \end{cases} \tag{55}$$

The matrices $[\Gamma],[\lambda]$ are given by:

$$[\Gamma] = \begin{bmatrix} [\Gamma^{(1)}] & [0] & [0] & [0] \\ [0] & [\Gamma^{(1)}]^T & [0] & [0] \\ [0] & [0] & [\Gamma^{(2)}] & [0] \\ [0] & [0] & [0] & [\Gamma^{(2)}]^T \end{bmatrix} \quad \text{where} \quad [\Gamma^{(1)}] = \begin{bmatrix} \Gamma_{11}^{(1)} & \Gamma_{12}^{(1)} \\ -\Gamma_{12}^{(1)} & \Gamma_{11}^{(1)} \end{bmatrix},\ [\Gamma^{(2)}] = \begin{bmatrix} \Gamma_{11}^{(2)} & \Gamma_{12}^{(2)} \\ -\Gamma_{12}^{(2)} & \Gamma_{11}^{(2)} \end{bmatrix} \tag{56}$$

$$[\lambda] = \begin{bmatrix} [\lambda^{(0)}] & [0] & [0] & [0] \\ [0] & [\lambda^{(0)}] & [0] & [0] \\ [0] & [0] & [\lambda^{(0)}] & [0] \\ [0] & [0] & [0] & [\lambda^{(0)}] \end{bmatrix} \quad \text{where} \quad [\lambda^{(0)}] = \begin{bmatrix} 1 & 0 \\ 0 & -1 \end{bmatrix} \tag{57}$$

$$\Gamma_{11}^{(1)} = \Gamma_{11}^{(2)} = \frac{\pi^2}{L^2},\ \Gamma_{12}^{(1)} = \Gamma_{12}^{(2)} = 0 \qquad \text{for } M_x$$

$$\Gamma_{11}^{(1)} = \frac{\left(\beta_1^2 - \alpha_1^2\right)}{R^2},\ \Gamma_{12}^{(1)} = -\frac{2\alpha_1\beta_1}{R^2},\ \Gamma_{11}^{(2)} = \frac{\left(\beta_2^2 - \alpha_2^2\right)}{R^2},\ \Gamma_{12}^{(2)} = -\frac{2\alpha_2\beta_2}{R^2} \qquad \text{for } M_\varphi$$

$$\left.\begin{aligned} \Gamma_{11}^{(1)} &= \frac{\left[\pi^4R^4\left(\beta_1^2 - \alpha_1^2\right) + 2L^2\pi^2R^2\left(\alpha_1^4 - 6\alpha_1^2\beta_1^2 + \beta_1^4\right) - L^4\left(\alpha_1^6 - 15\alpha_1^4\beta_1^2 + 15\alpha_1^2\beta_1^4 + \beta_1^6\right)\right]}{L^2\pi^2R^5}, \\ \Gamma_{12}^{(1)} &= -\frac{2\alpha_1\beta_1\left[\pi^2R^2 - L^2\left(\alpha_1^2 - 3\beta_1^2\right)\right]\left[\pi^2R^2 + L^2\left(\beta_1^2 - 3\alpha_1^2\right)\right]}{L^2\pi^2R^5}, \\ \Gamma_{11}^{(2)} &= \frac{\left[\pi^4R^4\left(\beta_2^2 - \alpha_2^2\right) + 2L^2\pi^2R^2\left(\alpha_2^4 - 6\alpha_2^2\beta_2^2 + \beta_2^4\right) - L^4\left(\alpha_2^6 - 15\alpha_2^4\beta_2^2 + 15\alpha_2^2\beta_2^4 + \beta_2^6\right)\right]}{L^2\pi^2R^5}, \\ \Gamma_{12}^{(2)} &= -\frac{2\alpha_2\beta_2\left[\pi^2R^2 - L^2\left(\alpha_2^2 - 3\beta_2^2\right)\right]\left[\pi^2R^2 + L^2\left(\beta_2^2 - 3\alpha_2^2\right)\right]}{L^2\pi^2R^5} \end{aligned}\right\} \qquad \text{for } N_x \tag{58}$$

$$\left.\begin{aligned} &\Gamma_{11}^{(1)} = \frac{\left[\pi^4R^4 + 2L^2\pi^2R^2\left(\beta_1^2 - \alpha_1^2\right) + L^4\left(\alpha_1^4 - 6\alpha_1^2\beta_1^2 + \beta_1^4\right)\right]}{L^4R^3},\ \Gamma_{12}^{(1)} = -\frac{4\alpha_1\beta_1\left[L^2\left(\beta_1^2 - \alpha_1^2\right) + \pi^2R^2\right]}{L^4R^3}, \\ &\Gamma_{11}^{(2)} = \frac{\left[\pi^4R^4 + 2L^2\pi^2R^2\left(\beta_2^2 - \alpha_2^2\right) + L^4\left(\alpha_2^4 - 6\alpha_2^2\beta_2^2 + \beta_2^4\right)\right]}{L^4R^3},\ \Gamma_{12}^{(2)} = -\frac{4\alpha_2\beta_2\left[L^2\left(\beta_2^2 - \alpha_2^2\right) + \pi^2R^2\right]}{L^4R^3} \end{aligned}\right\} \qquad \text{for } N_\varphi$$

$$\Gamma_{11}^{(1)} = -\frac{\alpha_1\pi}{RL}, \quad \Gamma_{12}^{(1)} = -\frac{\beta_1\pi}{RL}, \quad \Gamma_{11}^{(2)} = -\frac{\alpha_2\pi}{RL}, \quad \Gamma_{12}^{(2)} = -\frac{\beta_2\pi}{RL} \quad \text{for } M_{x\varphi}$$

$$\left.\begin{aligned}
\Gamma_{11}^{(1)} &= \frac{\alpha_1\left[\pi^4R^4 - 2L^2\pi^2R^2\left(\alpha_1^2 - 3\beta_1^2\right) + L^4\left(\alpha_1^4 - 10\alpha_1^2\beta_1^2 + 5\beta_1^4\right)\right]}{L^3\pi R^4} \\
\Gamma_{12}^{(1)} &= \frac{\beta_1\left[\pi^4R^4 + 2L^2\pi^2R^2\left(\beta_1^2 - 3\alpha_1^2\right) + L^4\left(5\alpha_1^4 - 10\alpha_1^2\beta_1^2 + \beta_1^4\right)\right]}{L^3\pi R^4} \\
\Gamma_{11}^{(2)} &= \frac{\alpha_2\left[\pi^4R^4 - 2L^2\pi^2R^2\left(\alpha_2^2 - 3\beta_2^2\right) + L^4\left(\alpha_2^4 - 10\alpha_2^2\beta_2^2 + 5\beta_2^4\right)\right]}{L^3\pi R^4} \\
\Gamma_{12}^{(2)} &= \frac{\beta_2\left[\pi^4R^4 + 2L^2\pi^2R^2\left(\beta_2^2 - 3\alpha_2^2\right) + L^4\left(5\alpha_2^4 - 10\alpha_2^2\beta_2^2 + \beta_2^4\right)\right]}{L^3\pi R^4}
\end{aligned}\right\} \text{ for } N_{x\varphi} \tag{59}$$

$$\left.\begin{aligned}
\Gamma_{11}^{(1)} &= \frac{\pi\left[\pi^2R^2 + L^2\left(\beta_1^2 - \alpha_1^2\right)\right]}{L^3R^2}, \quad \Gamma_{12}^{(1)} = \frac{-2\alpha_1\beta_1\pi}{LR^2} \\
\Gamma_{11}^{(2)} &= \frac{\pi\left[\pi^2R^2 + L^2\left(\beta_2^2 - \alpha_2^2\right)\right]}{L^3R^2}, \quad \Gamma_{12}^{(2)} = -\frac{2\alpha_2\beta_2\pi}{LR^2}
\end{aligned}\right\} \text{ for } Q_x$$

$$\left.\begin{aligned}
\Gamma_{11}^{(1)} &= \frac{\alpha_1\left[\pi^2R^2 - L^2\left(\alpha_1^2 - 3\beta_1^2\right)\right]}{L^2R^3}, \quad \Gamma_{12}^{(1)} = \frac{\beta_1\left[\pi^2R^2 + L^2\left(\beta_1^2 - 3\alpha_1^2\right)\right]}{L^2R^3} \\
\Gamma_{11}^{(2)} &= \frac{\alpha_2\left[\pi^2R^2 - L^2\left(\alpha_2^2 - 3\beta_2^2\right)\right]}{L^2R^3}, \quad \Gamma_{12}^{(2)} = \frac{\beta_2\left[\pi^2R^2 + L^2\left(\beta_2^2 - 3\alpha_2^2\right)\right]}{L^2R^3}
\end{aligned}\right\} \text{ for } Q_\varphi \tag{60}$$

An open barrel reinforced concrete cylindrical shell with geometric properties given in Table 1 is analyzed under uniform surface load varying sinusoidally in addition to the sinusoidal symmetric edge loads namely: i) fixed unitary moment; ii) unit axial edge load; and iii) unit shear edge load, considered to act one-by-one successively along the longitudinal boundaries. Figures 4-5 show the stress resultants obtained from the analysis using proposed close form expressions, for different values of φ. It can be seen from the figures that stress resultants are symmetric with respect to the crown of the shell and qualitatively similar under different edge loads. It is also seen that the obtained results on the basis of proposed expressions closely agree with those obtained from the detailed FEM analysis based on the procedures discussed by Stanley and Huges (1984). The stress resultants obtained from detailed FEM analysis are shown in Figure 6, for comparison.

Table 1 Geometric properties of the RC shell (case i)

Description	values
Φ_k	45°
L	26.67m
R	8m
t	80mm
Concrete Mix and steel grade	M_{25} and Fe 415 steel
Dead load	25 x 0.08 = 2.0 kN/m^2
Live load for inspection	0.5 kN/m^2
Load due to finishes	0.75 kN/m^2
Total load	3.25 kN/m^2
Young's modulus of concrete, E	25 x 10^6 kN/m^2
Poisson's ratio of concrete, ν	0.20

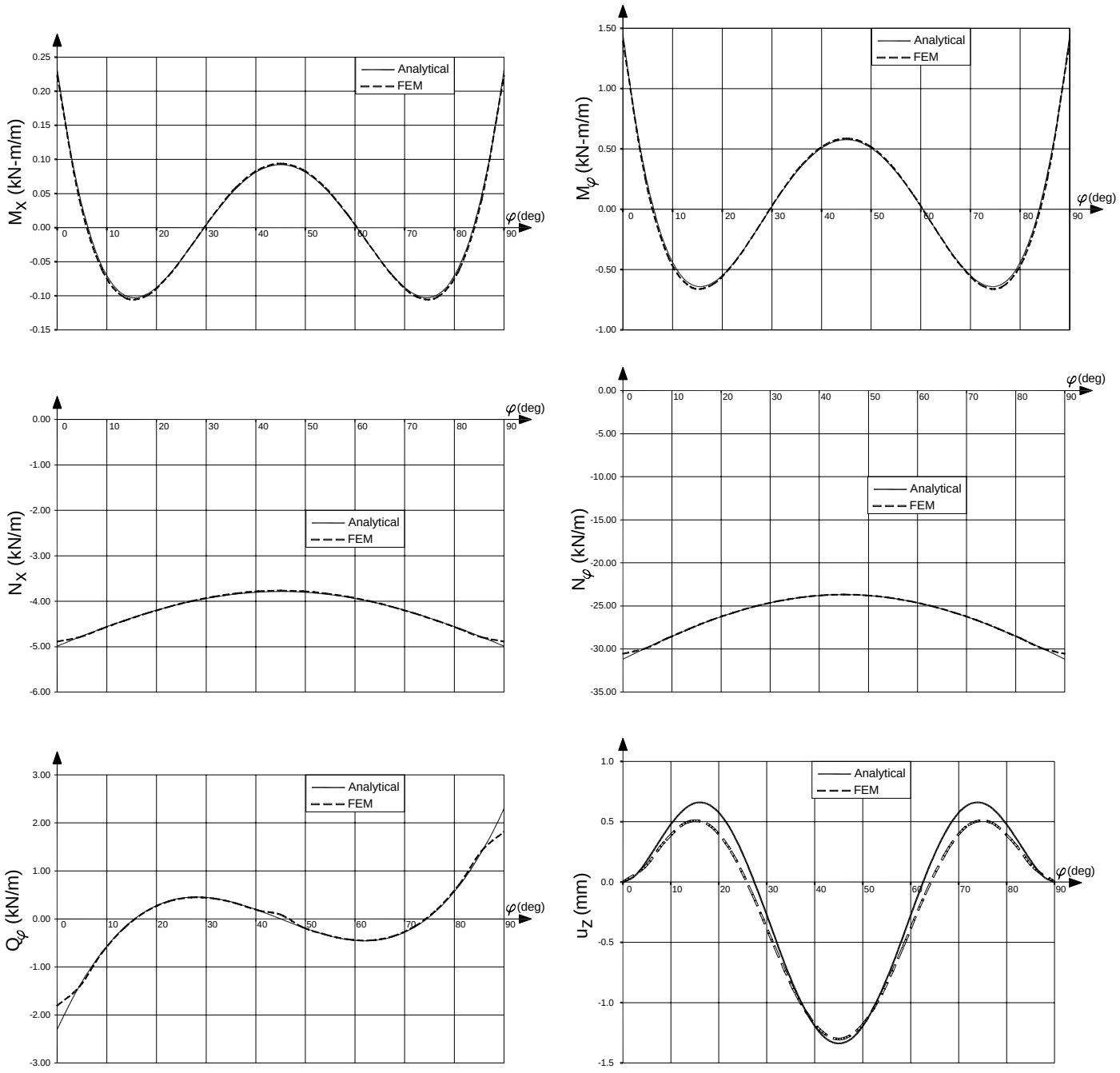

Figure 4. Stress resultants for RC shell at φ = 45º

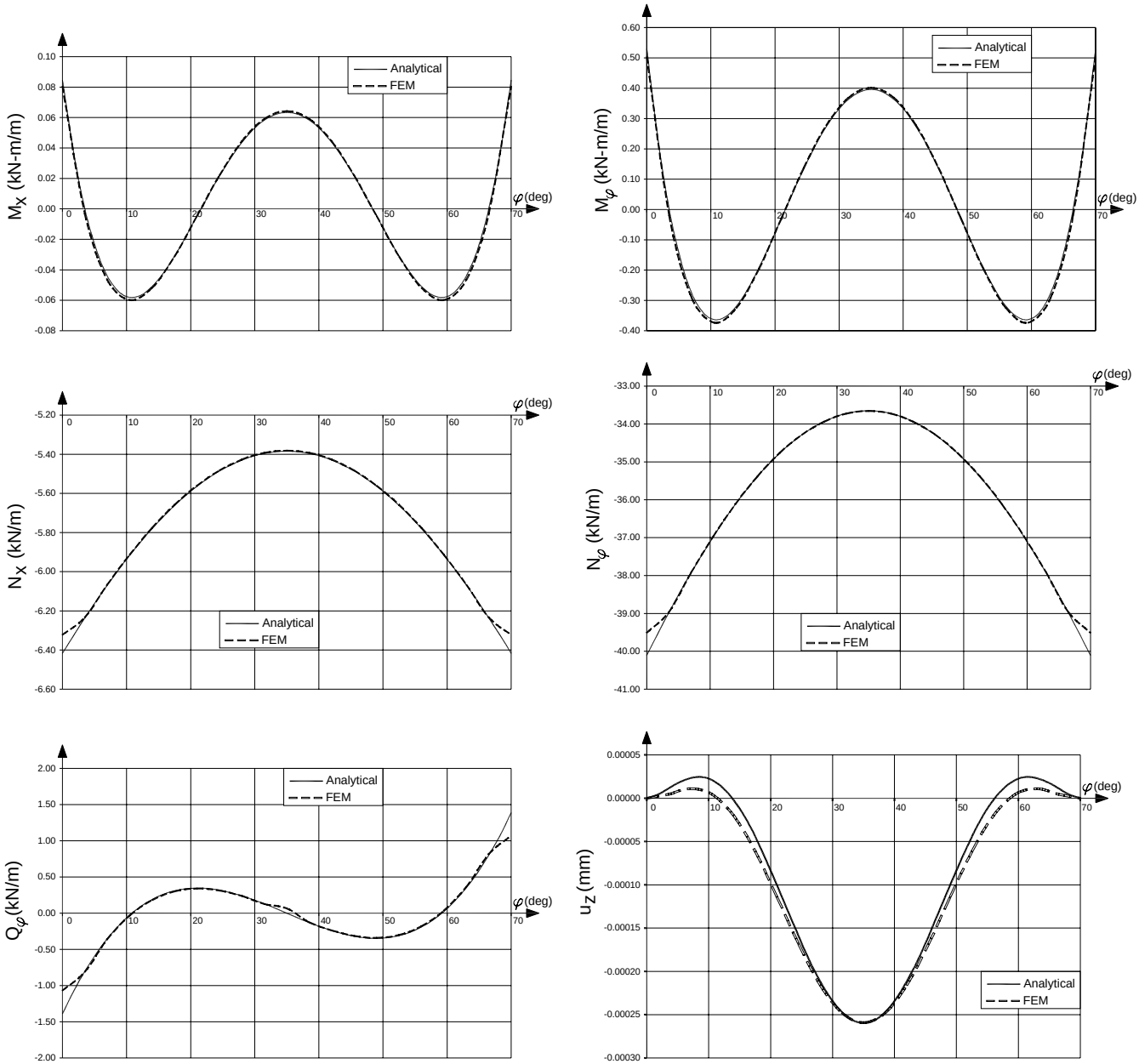

Figure 5. Stress resultants for RC shell at φ = 35º

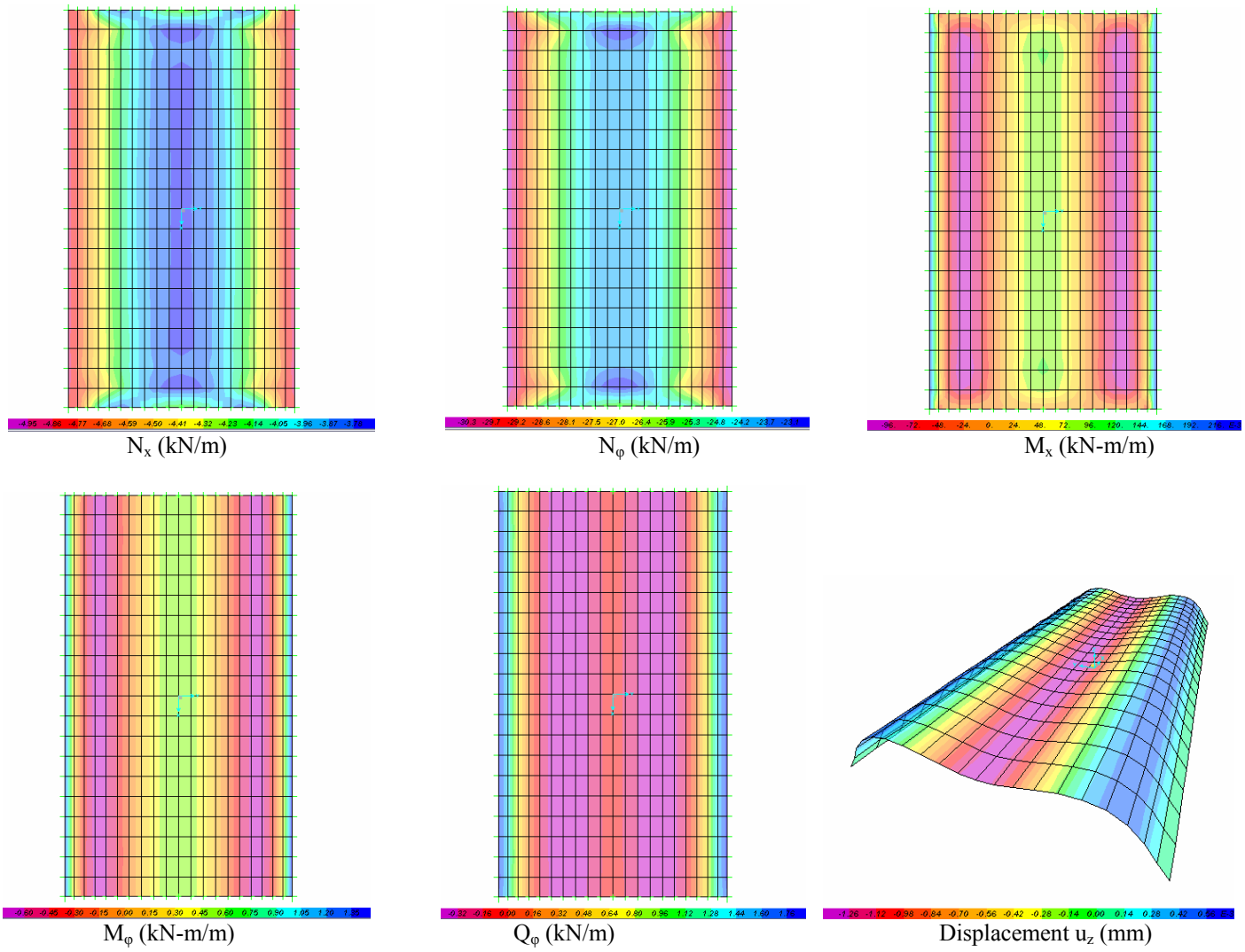

Figure 6. Stress resultants and displacement of RC shell obtained from FEM at φ = 45º

3.3 Design charts

After satisfactory comparison of stress resultants and displacement of RC shells obtained by employing the proposed expressions with that of detailed FEM, RC shell is now analyzed for different R/L ratios and angles of curvature to obtain Design charts for closer intervals of φ while Table 2 shows the stress resultants for edge loads. Based on classical flexural theory, using the proposed expressions in close form, Design charts are developed for computing the stress resultants in open cylindrical shells with varying geometric parameters. Figures 7-9 show the proposed Design charts plotted for different R/L ratios for practical cases of R/t and Φ angles those can be readily used for analyzing the shells without undergoing detailed computations. The expressions are also proposed in closed form for analysis of RC shells under sinusoidal surface load in addition to unit edge loads of different types. It is seen from the design curves that they follow the same trend for all edge load cases namely: i) fixed moment couple along longitudinal edge; ii) axial load along the longitudinal edge; as well as iii) shear edge load. The design curves can be readily used to obtain the stress resultants for RC open barrel cylindrical shell for varying R/L values. The stress resultants can also be obtained for any desired values of φ that can be necessary for detailing of reinforcement, particularly near the crown and the valley. The numerical problem solved using the design charts show computation of final stress resultants at closer intervals of Φ. Results obtained closely agree with that of the results obtained through finite element analysis. The proposed design curves shall be readily used in design offices that do not have access to high end software. Further, they shall also serve as an easy checking tool for assessing the correctness of the results given by the software. The proposed design curves shall enable the design engineers to understand the qualitative range of deviation, if any, from the results given by the software.

Table 2 Stress resultants of RC shell under sinusoidal surface load and different edge loads (case ii)

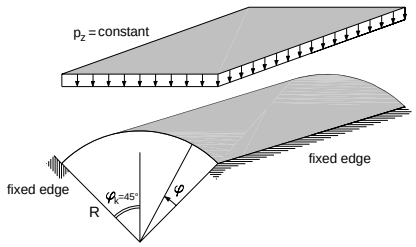 Shells under uniform distribued load						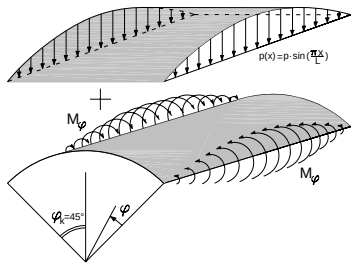 Surface load + moment edge load					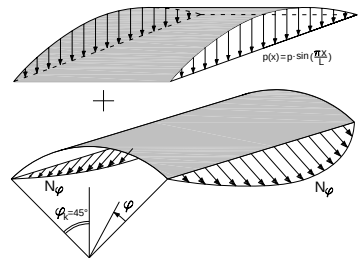 Surface load + axial edge load					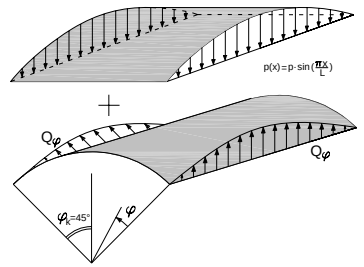 Surface load + shear edge load				
f	N_x	N_f	M_x	M_f	Q_f	N_x	N_f	M_x	M_f	Q_f	N_x	N_f	M_x	M_f	Q_f	N_x	N_f	M_x	M_f	Q_f
(deg)	(kN/m)	(kN/m)	(kN-m/m)	(kN-m/m)	(kN/m)	(kN/m)	(kN/m)	(kN-m/m)	(kN-m/m)	(kN/m)	(kN/m)	(kN/m)	(kN-m/m)	(kN-m/m)	(kN/m)	(kN/m)	(kN/m)	(kN-m/m)	(kN-m/m)	(kN/m)
0	-4.988	-31.177	0.231	1.447	-2.298	1283.62	0.000	2.237	1.000	0.000	1372.76	1.00	2.52	0.00	0.00	1482.95	0.00	2.98	0.00	-1.00
10	-4.560	-28.499	-0.070	-0.439	-0.566	181.59	-8.464	1.506	-0.445	-2.947	176.91	-8.13	1.67	-1.44	-3.09	153.08	-9.82	1.93	-2.50	-3.87
20	-4.199	-26.247	-0.088	-0.549	0.278	-218.88	-24.066	0.795	-4.875	-4.042	-241.31	-24.44	0.86	-5.99	-4.19	-277.95	-26.46	0.96	-7.76	-4.66
30	-3.940	-24.625	0.004	0.023	0.449	-261.97	-35.258	0.216	-9.511	-3.164	-271.41	-35.80	0.22	-10.73	-3.25	-274.24	-37.25	0.20	-12.83	-3.44
40	-3.804	-23.778	0.081	0.507	0.197	-211.41	-40.322	-0.110	-12.285	-1.164	-206.95	-40.77	-0.14	-13.55	-1.19	-180.18	-41.57	-0.22	-15.74	-1.23
50	-3.804	-23.778	0.081	0.507	-0.197	-211.41	-40.322	-0.110	-12.285	1.164	-206.95	-40.77	-0.14	-13.55	1.19	-180.18	-41.57	-0.22	-15.74	1.23
60	-3.940	-24.625	0.004	0.023	-0.449	-261.97	-35.258	0.216	-9.511	3.164	-271.41	-35.80	0.22	-10.73	3.25	-274.24	-37.25	0.20	-12.83	3.44
70	-4.199	-26.247	-0.088	-0.549	-0.278	-218.88	-24.066	0.795	-4.875	4.042	-241.31	-24.44	0.86	-5.99	4.19	-277.95	-26.46	0.96	-7.76	4.66
80	-4.560	-28.499	-0.070	-0.439	0.566	181.59	-8.464	1.506	-0.445	2.947	176.91	-8.13	1.67	-1.44	3.09	153.08	-9.82	1.93	-2.50	3.87
90	-4.988	-31.176	0.231	1.447	2.298	1283.62	0.000	2.237	1.000	0.000	1372.76	1.00	2.52	0.00	0.00	1482.95	0.00	2.98	0.00	1.00

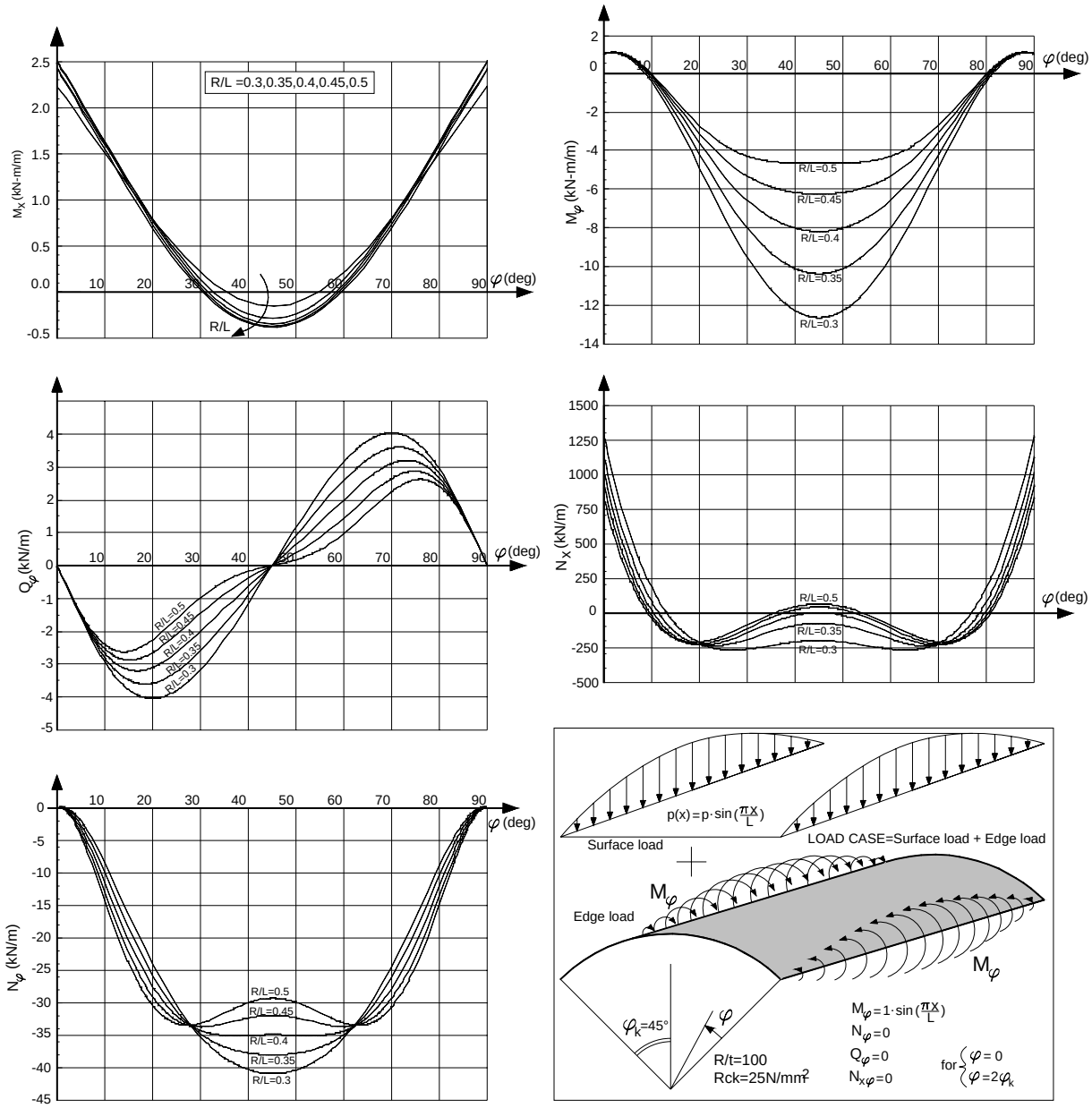

Figure 7. Design charts for RC shells under surface load and moment edge loads

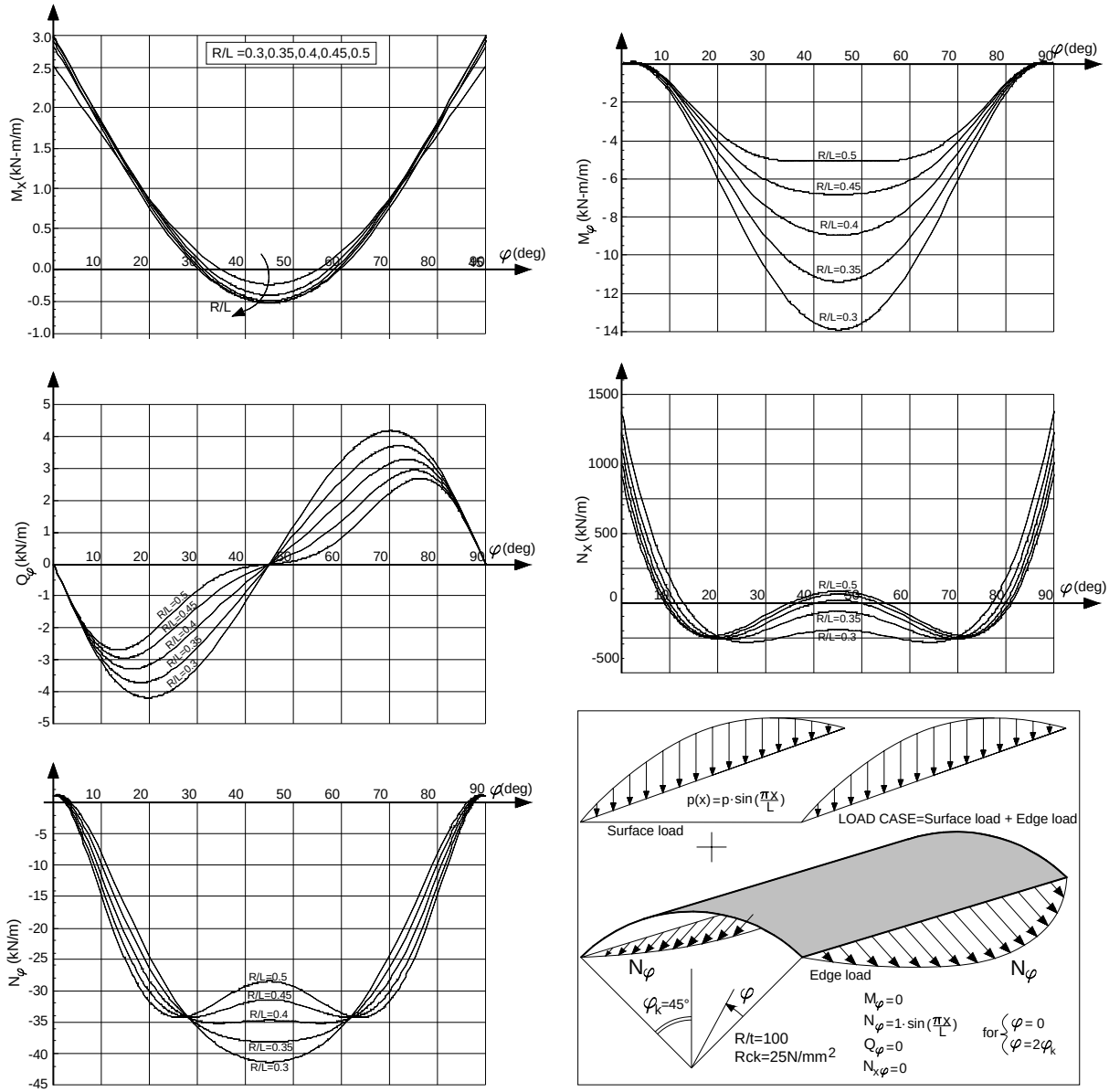

Figure 8. Design charts for RC shells under surface load and axial edge loads

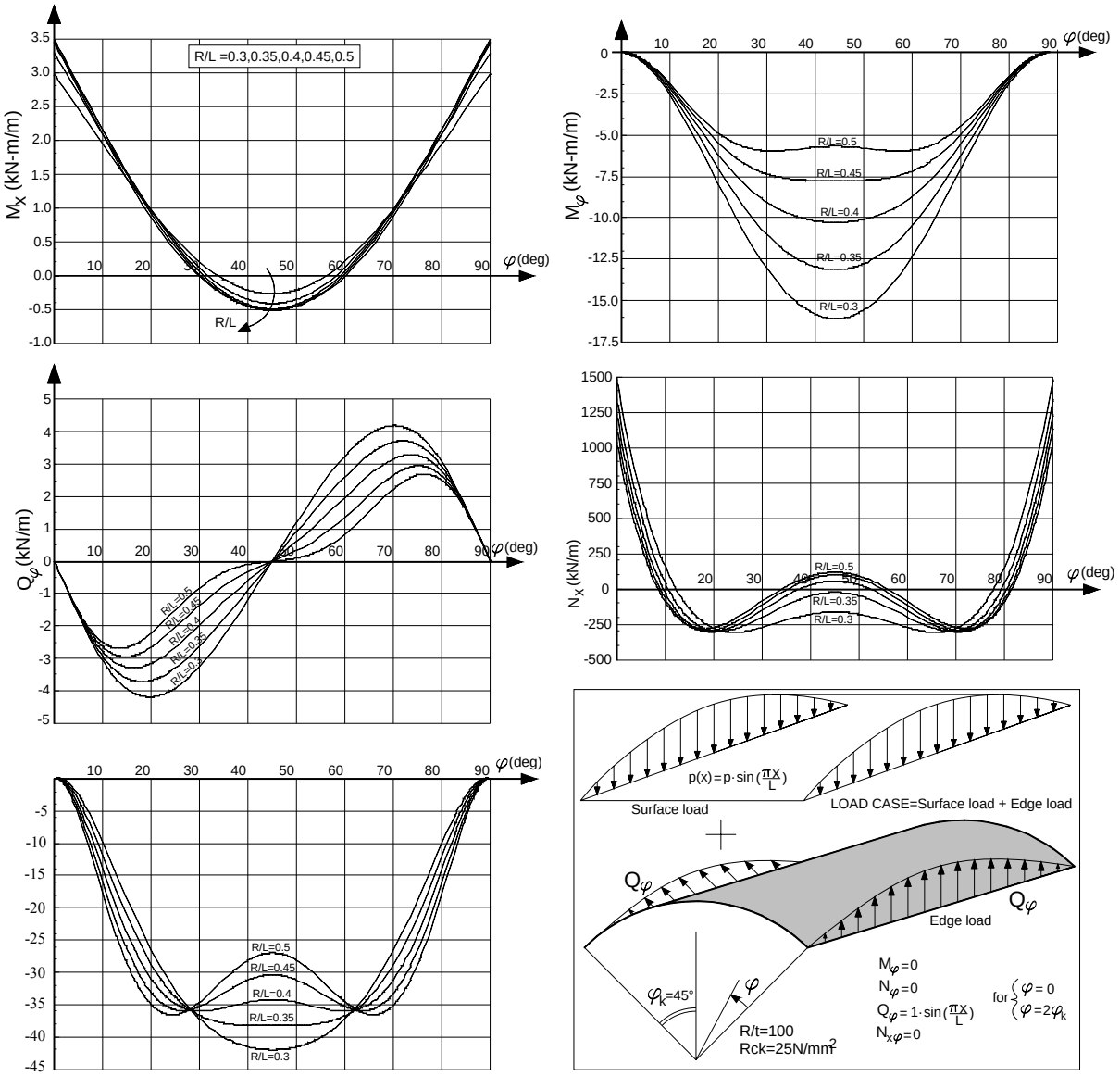

Figure 9. Design charts for RC shells under surface load and shear edge loads

4. Axial force-bending moment interaction

Concrete under multi-axial compressive stress state exhibits significant nonlinearity that can be successfully represented by nonlinear constitutive models capable of handling inelastic deformations and cyclic loading. Further, it is necessary to describe a suitable failure criterion for complete description of ultimate strength. A reinforced concrete element of rectangular cross-section is studied for axial force-bending moment yield interaction behaviour for different percentage of tension and compression reinforcements (Chandrasekaran *et al.* 2009). Bernoulli hypothesis of linear strain over the cross-section, both for elastic and elastic-plastic responses of the element, under bending moment combined with axial force was assumed. The interaction behaviour becomes critical when one of the following conditions apply namely: i) strain in reinforcing steel in tension reaches ultimate limit; ii) strain in concrete in extreme compression fibre reaches ultimate limit; as well as iii) maximum strain in concrete in compression reaches elastic limit under only axial compression. Axial force-bending moment limit domain consisting of six sub-domains are described; collapse in sub-domains (1) and (2) is caused by yielding of steel whereas for sub-domains (3) to (6), the collapse is caused by crushing of concrete. Table 3 gives the resume of expressions for various sub-domains, as reported by the researchers; in general terms, axial force-bending moment interaction can be expressed as below:

$$\begin{cases} N_{\varphi u}(x_c) = \int_{A_c} b\,\sigma_c(\varepsilon_c(y))dy - \sigma_{st}A_{st} + \sigma_{sc}A_{sc} \\ M_{\varphi u}(x_c) = \int_{A_c} b\,\sigma_c(\varepsilon_c(y))\left(\frac{D}{2}-y\right)dy + (\sigma_{st}A_{st} + \sigma_{sc}A_{sc})\left(\frac{D}{2}-d\right) \end{cases} \tag{61}$$

where A_c is the area of concrete in compression; if the section is in full tension, the integral vanishes as the neutral axis is negative. For the neutral axis greater than the depth of the section, say in this case, thickness of the shell, the integral shall extend for the total thickness of the shell. In general, as the shell remains in compression, the depth of neutral axis is always greater than the thickness of the shell. Figure 10 shows the cross-section element of the shell; axial force normal to the section, N_φ and moment about the section, M_φ are now considered for studying the interaction. The stress resultants ($N_{\varphi e,}$ $M_{\varphi e}$) are determined from the proposed equations (case i) presented above and the values are plotted in the P-M domain. Points A to E correspond to shells with different values of φ_k. It can be seen that the stress resultants lie in the sub-domain (3) for all values of φ_k indicating a compression failure initiated by crushing of concrete. For the failure point on the P-M boundary, for example, A', following equation holds good:

$$N_{\varphi u}(x_c) - \frac{N_{\varphi e}}{M_{\varphi e}} M_{\varphi u}(x_c) = 0 \tag{62}$$

By iteration, Eq. (62) is solved for x_c and further by substitution, ($N_{\varphi u,}$ $M_{\varphi u}$) are determined using Eq. (30). Depths of neutral axis thus obtained for different angles of curvature and the corresponding points on the P-M boundary namely: A' to E' are shown in Figure 9. Factor of safety (F.S) is obtained from the following relationship:

$$F.S = \frac{A'O}{AO} \tag{63}$$

Using the above equation, factor of safety for shells with different φ_k are computed and shown in Figure 10. It can be seen from the figure that factor of safety reduces with increase in angle of curvature of the shell. Also, strain in concrete, for all cases, reaches ultimate limit prompting a compression failure while those in tension and compression steel are within the yield limits. The failure points interpreted on the P-M domain show compression failure of shell section initiating crushing of concrete.

Table 3. Resume of expressions for P-M interaction (Chandrasekaran *et. al. 2009*)

sub-domain	x_c	$q(x_c)$	$\varepsilon_{c,max}(x_c)$	$\varepsilon_{st}(x_c)$	$\varepsilon_{sc}(x_c)$	$P_u(x_c)$	$M_u(x_c)$
(1)	$]-\infty,0]$	0	$\frac{\varepsilon_{su}x_c}{D-x_c-d}$	ε_{su}	$\varepsilon_{su}\left(\frac{x_c-d}{D-x_c-d}\right)$	$P_{u,st}$	$M_{u,st}$
(2a)	$[0,x_c']$	0	$\frac{\varepsilon_{su}x_c}{D-x_c-d}$	ε_{su}	$\varepsilon_{su}\left(\frac{x_c-d}{D-x_c-d}\right)$	$P_{u,st}+P_{u1,con}(q=0)$	$M_{u,st}+M_{u1,con}(q=0)$
(2b)	$[x_c',x_c'']$	$x_c-\frac{\varepsilon_{c0}}{\varepsilon_{su}}(D-x_c-d)$	$\frac{\varepsilon_{su}x_c}{D-x_c-d}$	ε_{su}	$\varepsilon_{su}\left(\frac{x_c-d}{D-x_c-d}\right)$	$P_{u,st}+P_{u1,con}$	$M_{u,st}+M_{u1,con}$
(3)	$[x_c'',x_c''']$	$\frac{\varepsilon_{cu}-\varepsilon_{c0}}{\varepsilon_{cu}}x_c$	ε_{cu}	$\frac{\varepsilon_{cu}(D-x_c-d)}{x_c}$	$\frac{\varepsilon_{cu}(x_c-d)}{x_c}$	$P_{u,st}+P_{u1,con}$	$M_{u,st}+M_{u1,con}$
(4)	$[x_c''',D-d]$	$\frac{\varepsilon_{cu}-\varepsilon_{c0}}{\varepsilon_{cu}}x_c$	ε_{cu}	$\frac{\varepsilon_{cu}(D-x_c-d)}{x_c}$	$\frac{\varepsilon_{cu}(x_c-d)}{x_c}$	$P_{u,st}+P_{u1,con}$	$M_{u,st}+M_{u1,con}$
(5)	$[D-d,D]$	$\frac{\varepsilon_{cu}-\varepsilon_{c0}}{\varepsilon_{cu}}x_c$	ε_{cu}	$\frac{\varepsilon_{cu}(D-x_c-d)}{x_c}$	$\frac{\varepsilon_{cu}(x_c-d)}{x_c}$	$P_{u,st}+P_{u1,con}$	$M_{u,st}+M_{u1,con}$
(6)	$[D,+\infty[$	$\frac{\varepsilon_{cu}-\varepsilon_{c0}}{\varepsilon_{cu}}D$	$\frac{\varepsilon_{cu}\varepsilon_{c0}x_c}{\varepsilon_{cu}x_c-D(\varepsilon_{cu}-\varepsilon_{c0})}$	$\frac{\varepsilon_{cu}\varepsilon_{c0}(D-x_c-d)}{\varepsilon_{cu}x_c-D(\varepsilon_{cu}-\varepsilon_{c0})}$	$\frac{\varepsilon_{cu}\varepsilon_{c0}(x_c-d)}{\varepsilon_{cu}x_c-D(\varepsilon_{cu}-\varepsilon_{c0})}$	$P_{u,st}+P_{u1,con}+P_{u2,con}$	$M_{u,st}+M_{u1,con}+M_{u2,con}$

$$\varepsilon_{c,max}(x_c)=\varepsilon_c(x_c,y=0) \qquad P_{u,st}=A_{sc}\sigma_{sc}-A_{st}\sigma_{st}=b(D-d)(p_c\sigma_{sc}-p_t\sigma_{st})$$

$$M_{u,st}=(A_{sc}\sigma_{sc}-A_{st}\sigma_{st})\left(\frac{D}{2}-d\right)=b(D-d)(p_c\sigma_{sc}-p_t\sigma_{st})\left(\frac{D}{2}-d\right)$$

$$P_{u1,con}=bq\sigma_{c0}+\frac{b\sigma_{c0}\varepsilon_{c,max}(q-x_c)^2}{3x_c^2\varepsilon_{c0}^2}\left[3\varepsilon_{c0}x_c+\varepsilon_{c,max}(q-x_c)\right]$$

$$M_{u1,con}=\frac{bq\sigma_{c0}}{2}(D-q)-\frac{b\sigma_{c0}\varepsilon_{c,max}(q-x_c)^2}{12x_c^2\varepsilon_{c0}^2}\left[2\varepsilon_{c0}x_c(4q+2x_c-3D)+\varepsilon_{c,max}(q-x_c)(x_c+3q-2D)\right]$$

$$P_{u2,con}=-\frac{b\sigma_{c0}\varepsilon_{c,max}\left[3\varepsilon_{c0}x_c+\varepsilon_{c,max}(D-x_c)\right](D-x_c)^2}{3x_c^2\varepsilon_{c0}^2}$$

$$M_{u2,con}=\frac{b\sigma_{c0}\varepsilon_{c,max}(D-x_c)^2\left[2\varepsilon_{c0}x_c(D+2x_c)+\varepsilon_{c,max}(D^2-x_c^2)\right]}{12x_c^2\varepsilon_{c0}^2}$$

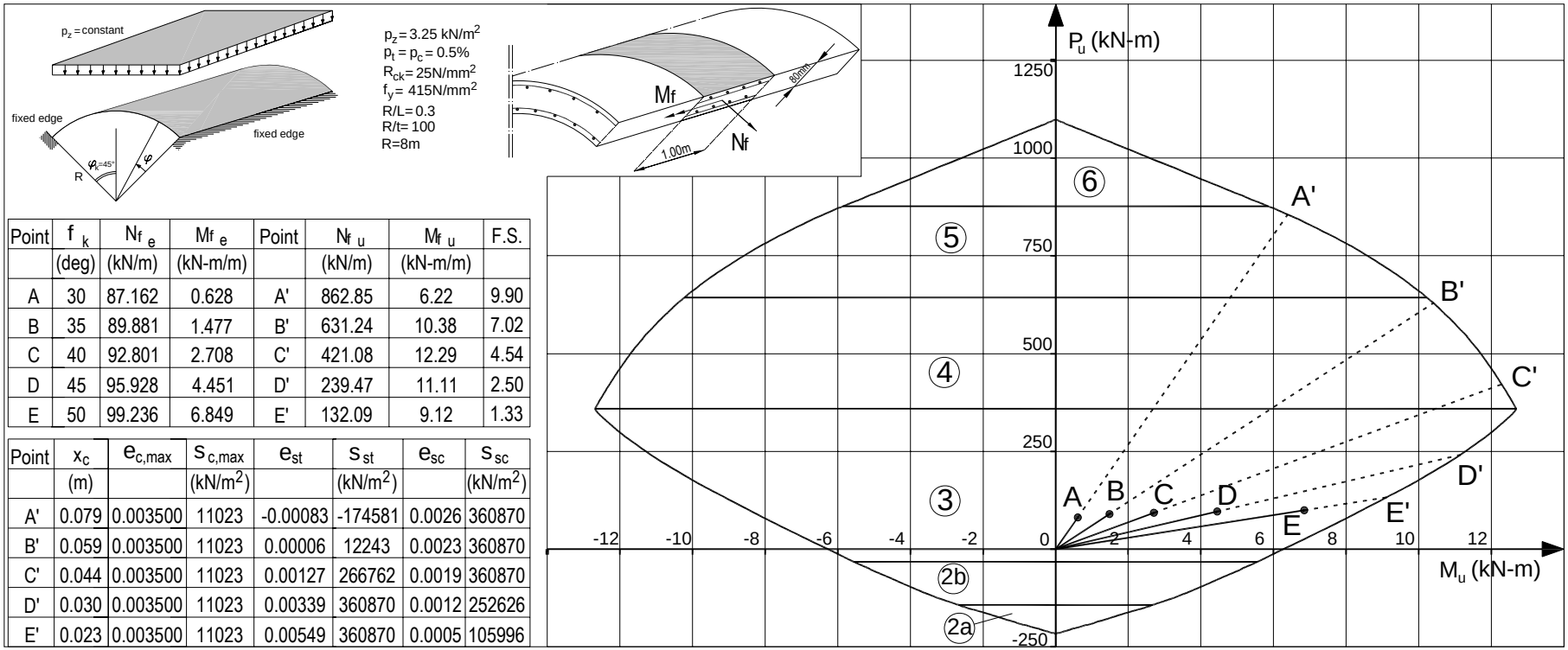

Point	f_k	$N_{f\,e}$	$M_{f\,e}$	Point	$N_{f\,u}$	$M_{f\,u}$	F.S.
	(deg)	(kN/m)	(kN-m/m)		(kN/m)	(kN-m/m)	
A	30	87.162	0.628	A'	862.85	6.22	9.90
B	35	89.881	1.477	B'	631.24	10.38	7.02
C	40	92.801	2.708	C'	421.08	12.29	4.54
D	45	95.928	4.451	D'	239.47	11.11	2.50
E	50	99.236	6.849	E'	132.09	9.12	1.33

Point	x_c	$e_{c,max}$	$s_{c,max}$	e_{st}	s_{st}	e_{sc}	s_{sc}
	(m)		(kN/m²)		(kN/m²)		(kN/m²)
A'	0.079	0.003500	11023	-0.00083	-174581	0.0026	360870
B'	0.059	0.003500	11023	0.00006	12243	0.0023	360870
C'	0.044	0.003500	11023	0.00127	266762	0.0019	360870
D'	0.030	0.003500	11023	0.00339	360870	0.0012	252626
E'	0.023	0.003500	11023	0.00549	360870	0.0005	105996

Figure 10. Axial force-bending moment interaction of RC shells under uniformly distributed surface loads (P-M interaction)

5. Conclusions

Design curves for stress resultants based on the classical flexural theory for single barrel open cylindrical shells are presented with analytical expressions in closed form. The effect of variation of angle of curvature of shell geometry on the final stress resultants is demonstrated using the proposed design curves. Plots of axial force-bending moment values on the P-M domain are illustrated to show the compression failure in RC shells initiated by crushing of concrete. As the behavior of the plots for various values of R/L is nonlinear, interpolations for still closer values of fraction of R/L is not recommended.

Common theories adopted for analysis of cylindrical shells interpret the design behavior in different ways. Therefore every design procedure developed without undergoing rigorous analysis leads to simple and close form solution but of course with some defects. Despite shell structures possess inherent advantages gained by its structural form, they are not very common due to their analysis complexities. Current study attempts to make shell analysis easy, popular and develops confidence in design offices, encouraging the designer to handle a complex problem through a simple graphical tool. With the use of proposed Design charts, stress resultants can be readily determined at the valley, crown or at any desired section for various type of edge loads. In the present context of design offices highly influenced by use of software, this study is an attempt in the direction of developing simple graphical tools based on well established theories so that the designer is sure to know the error, if committed both qualitatively and quantitatively.

Nomenclature

R	radius (m)	L	length (m)
φ_k	angle of the shell (deg)	t	thickness of the shell (mm)
E	Young's modulus of concrete (kN/m^2)	ν	Poisson's ratio of concrete
φ	generic angle in shell (deg)		
M_x	Bending moment in plane x-z	M_φ	Bending moment in plane r-φ
$M_{x\varphi}$	Torque moment in plane x-z	$M_{\varphi x}$	Torque moment in plane r-φ
N_x	Axial force in x-direction	N_φ	Axial force in φ-direction
$N_{x\varphi}$	Shear force in x –direction		
Q_x	Shear force in radial direction along longitudinal edges		
Q_φ	Shear force in radial direction along transversal edges		
ε_x	normal strain in x-direction	ε_φ	normal strain in φ-direction
$\gamma_{x\varphi}$	shear strain in plane x-φ	ϕ_x	curvature in plane x-z
ϕ_φ	curvature in plane r-φ	$\phi_{x\varphi}$	curvature in plane x-z
p_x	surface load on the shell in x-direction (kN/m^2)	p_φ	surface load in φ-direction (kN/m^2)
p_r	surface load on the shell in radial direction (kN/m^2)	p_z	surface load on the shell in z-direction (kN/m^2)
u_x	displacement component in x-direction	u_φ	displacement component in φ-direction
u_r	displacement component in radial direction	u_z	displacement component in z- direction
∇^8	differential operator of eight order	∇^4	differential operator of fourth order
d	effective cover of the section (m)		
x_c	depth of neutral axis measure from extreme compression fibre (mm)		
$x_c^0, x_c', x_c'', x_c'''$	limit position neutral axis (mm)	q	depth of plastic kernel of concrete (mm)
y	depth of generic fibre of concrete measured from extreme compression fibre (mm)		
ε_c	strain in generic fibre of concrete	$\varepsilon_{c,max}$	maximum strain in concrete
ε_{c0}	elastic limit strain in concrete	ε_{cu}	ultimate limit strain in concrete
ε_{st}	strain in tensile reinforcement	ε_{sc}	strain in compression reinforcement
ε_{s0}	elastic limit strain in reinforcement	ε_{su}	ultimate limit strain in reinforcement
E_s	modulus of elasticity in steel (kN/m^2)	R_{ck}	compressive cube strength of concrete (kN/m^2)
σ_c	stress in generic fibre of concrete (kN/m^2)	$\sigma_{c,max}$	maximum stress in concrete (kN/m^2)
σ_{c0}	design ultimate stress in concrete in compression (kN/m^2)		

σ_y	yield strength of steel (kN/m^2)	σ_{s0}	design ultimate stress in steel (kN/m^2)
σ_{st}	stress in tensile reinforcement (kN/m^2)	σ_{sc}	stress in compression reinforcement (kN/m^2)
p_t	percentage of tensile reinforcement	p_c	percentage of compression reinforcement
A_{st}	area of tension reinforcement (m^2)	A_{sc}	area of compression reinforcement (m^2)
A_c	area of concrete in compression	F.S.	safety of safety in P-M interaction
$N_{\varphi e}$	Axial force in φ -direction in elastic range (kN)	$N_{\varphi u}$	Axial force in φ -direction at collapse (kN)
$M_{\varphi e}$	Bending moment in plane R-φ in elastic range (kN-m)	$M_{\varphi u}$	Moment in plane R-φ at collapse (kN-m)

References

Billington David P. 1965. *Thin shell concrete structures*. Mc-Graw Hill Inc.

Chandrasekaran, S., Ashutosh Srivastava, Parijat Naha. 2005. Computational tools for shell structures. *Proc. of Intl. conf. on structures and road transport (START-2005)*, IIT-Kharagpur, India, pp. 167-175.

Chandrasekaran, S., Srivastava, A. 2006. Design aids for multi-barrel RC cylindrical shells. *J. Struct. Engrg. SERC,* Vol. 33, No. 4, pp. 287-296.

Chandrasekaran S., Luciano Nunziante, Giorgio Serino, Federico Carannante 2009. *Seismic design aids for nonlinear analysis of reinforced concrete structures*. CRC Press, Taylor and Francis, Florida, USA, 246pp.

Flugge Wilhelm. 1967. *Stress in shells*. Springer Verlag, New York.

Ha-Wong Song, Sang-Hyo Shim, Keun-Joo Byun, Koichi Maekawa. 2002. Failure analysis of reinforced concrete shell structures using layered shell element with pressure node. *J. Struct. Engrg, ASCE*, Vol. 128, No. 5, pp. 655-664.

Jacques H., 1977. *Equilibrium of shell structures*. Clarendon press, Oxford.

Prabhakar G. 2003. Analysis of aircraft impact on containment structures. *Proc. of 5th Asia-Pacific conf. on Shocks and Impact loads on structures*, Hunan, China, pp. 315-322.

Ramaswamy G.S. 1968. *Design and construction of concrete shell roof*. First Edition, Mc-Graw Hill.

Rericha P. 1996. Local impact on RC shells and beams. *Proc. of International conf. on Structures under Shock and Impact loads (SUSI 96)*, Udine, Italy, No. 4, Computational Mechanics Publications, Southampton, pp. 341-349.

Stanley G.M., Huges T.T.R. 1984. Finite element procedures applicable to nonlinear analysis of RC shell structures. *Report ADA 146796, Defence Technology Information Center*, p. 68.

Timoshenko, S.P., Woinowsky-Krieger, S. 1959. *Theory of Plates and Shells.* 2d ed., McGraw-Hill Book Company, New York.

Wheen R.J, Anathraman. 1998. Concrete origami in Geodesic Domes, Conical tent and other Spatial Applications. *Proc. of IASS International Symposium on innovative applications of shells and spatial forms*. Bangalore, India, Nov. 21-25, Vol. 1.

Wheen R.J., Wheen P.R. 2003. A unique conical tent roof design and construction. *Proc. of 2nd Specialty conference on the conceptual approach to structural design*, Milan, Italy, pp.855-861.

Biographical notes

Prof. Srinivasan Chandrasekaran is Associate Professor in Department of Ocean Engineering, Indian Institute of Technology Madras, India. He has engaged in teaching and research activities since the last 20 years. His field of specialization is Structural dynamics and offshore structures. He has published several papers in various national, international conferences and journals and also recently published a book on seismic design aids, addressing latest concepts in seismic resistant design of RC structures. He is member of ASCE and several other national and international societies and reviewer of several international journals.

Prof. S.K.Gupta is working as Assistant Professor in Civil Engineering Department, Institute of Technology, Banaras Hindu University, India. He has done his research in the field of fluidized motion conveying of particulate solids. He has been in teaching and research for last 13 years and published over 15 papers in refereed international/ national journals and conferences. His research interest relates to the experimentation and modeling in the areas of multiphase flow, hydraulics, solar energy systems, and use of optimization techniques as well. He is a reviewer for an international journal published by Taylor and Francis and few other national journals.

Dr. Federico Carannante is a Lecturer on contract with Dept. of Structural Engineering, University of Naples Federico II, Naples, Italy. His research interest vests in functionally graded materials and their applications in structural health monitoring. He has about fifteen publications in refereed international journals and many conference publications to his credit.

Received October 2009
Accepted November 2009
Final acceptance in revised form December 2009